Electronic Supplementary Material (ESI) for Chemical Communications.

Asymmetric synthesis of optically active methyl-2-benzamido-methyl-3-hydroxy-butyrate by robust short-chain alcohol dehydrogenases from *Burkholderia gladioli*

Xiang Chen,[a,b] Zhi-Qiang Liu,[a,b] Jian-Feng Huang,[a,b] Chao-Ping Lin[a,b] and Yu-Guo Zheng*[a,b]

[a] *Institute of Bioengineering, Zhejiang University of Technology, Hangzhou 310014, China. Fax: +86-571-88320630; Tel: +86-571-88320630; E-mail: zhengyg@zjut.edu.cn*

[b] *Engineering Research Center of Bioconversion and Biopurification of Ministry of Education, Zhejiang University of Technology, Hangzhou 310014, China*

Supporting information

Table of Contents

1. General

Methyl 2-benzamido-methyl-3-oxobutyrate **29** and methyl-2-benzamido-methyl-3-hydroxy-butyrate (MBHB) were synthesized according to a modified literature procedure.[1] All the other chemicals were obtained from commercial suppliers, and used without further purification: N-(hydroxymethyl)benzamide (98%, Aldrich), phosphorus pentachloride (98%, Aladdin), (*Z*)-methyl 3-(pyrrolidin-1-yl)but-2-enoate (98%, Aldrich), acetaldehyde **1** (98%, Aladdin), butyraldehyde **2** (98%, Aladdin), benzaldehyde **3** (97%, Aladdin), 2,3-butanedione **4** (98%, Aladdin), 2-pentanone **5** (98%, Aladdin), 2-hexanone **6** (98%, Aladdin), cyclohexanone **7** (98%, Aladdin), 2-phenylcyclohexanone **8** (98%, Aladdin), 4-piperidone **9** (98%, Aladdin), acetophenone **10** (98%, Aladdin), (*R*)-1-phenylethanol (98%, Aladdin), 1-phenylethanol (98%, Aladdin), 4-methylacetophenone **11** (98%, Aladdin), (*R*)-1-(4-methylphenyl)ethanol (96%, Aladdin), 1-(4-methylphenyl)ethanol (96%, Aldrich), 4-methoxyacetophenone **12** (98%, Aladdin), (*R*)-1-(4-methoxyphenyl)ethanol (98%, Donggang Pharmaceutical Co., Ltd., China), 1-(4-methoxyphenyl)ethanol (98%, Aldrich), 2-methoxy acetophenone **13** (98%, Aladdin), (*R*)-1-(2-methoxyphenyl)ethanol (98%, Donggang Pharmaceutical Co., Ltd., China), 1-(2-methoxyphenyl)ethanol (98%, J&K Chemical Co., Ltd.), 3,5-dimethoxyacetophenone **14** (98%, Aldrich), (*S*)-1-(3,5-dimethoxyphenyl)ethanol (98%, Donggang Pharmaceutical Co., Ltd., China), 1-(3,5-dimethoxyphenyl)ethanol (98%, Donggang Pharmaceutical Co., Ltd., China), 4-fluoroacetophenone **15** (98%, Aladdin), (*S*)-1-(4-flourophenyl)ethanol (98%, Aladdin), 1-(4-flourophenyl)ethanol (98%, Aldrich), 4-trifluoromethyl acetophenone **16** (98%, Aladdin), (*S*)-1-(4-trifluoromethylphenyl)ethanol (98%, J&K Chemical Co., Ltd.), 1-(4-trifluoromethylphenyl)ethanol (98%, J&K Chemical Co., Ltd.), 3,5-bis(trifluoromethyl)

acetophenone **17** (98%, Aladdin), (*S*)-1-[3,5-bis(trifluoromethyl)phenyl]ethanol (98%, J&K Chemical Co., Ltd.), 1-[3,5-bis(trifluoromethyl)phenyl]ethanol (98%, Aladdin), 4-nitroacetophenone **18** (98%, Aladdin), (*S*)-1-(4-nitrophenyl)ethanol (98%, Donggang Pharmaceutical Co., Ltd., China), 1-(4-nitrophenyl)ethanol (98%, J&K Chemical Co., Ltd.), 1,2-diphenyl ethanedione **19** (98%, Aladdin), benzoylformic acid **20** (98%, J&K Chemical Co., Ltd.), (*S*)-α-hydroxy-benzeneacetic acid (98%, J&K Chemical Co., Ltd.), (*R*)-α-hydroxy-benzeneacetic acid (98%, J&K Chemical Co., Ltd.), 4-chloro-benzoylformic acid **21** (98%, Donggang Pharmaceutical Co., Ltd., China), (*S*)-4-chloro-α-hydroxy-benzeneacetic acid (98%, J&K Chemical Co., Ltd.), (*R*)-4-chloro-α-hydroxy-benzeneacetic acid (98%, J&K Chemical Co., Ltd.), 4-hydroxy-benzoylformic acid **22** (98%, Donggang Pharmaceutical Co., Ltd., China), (*S*)-α,4-dihydroxy-benzeneacetic acid (98%, J&K Chemical Co., Ltd.), (*R*)-α,4-dihydroxy-benzeneacetic acid (98%, J&K Chemical Co., Ltd.), ethyl acetoacetate **23** (98%, Aladdin), ethyl 3-hydroxybutyrate (98%, Aladdin), (*R*)-ethyl 3-hydroxybutyrate (98%, Aladdin), *t*-butyl acetoacetate **24** (98%, Aladdin), *t*-butyl 3-hydroxybutyrate (98%, Donggang Pharmaceutical Co., Ltd., China), (*S*)-*t*-butyl 3-hydroxybutyrate (98%, J&K Chemical Co., Ltd.), ethyl 4-chloroacetoacetate **25** (98%, Aldrich), ethyl (*S*)-4-chloro-3-hydroxybutyrate (98%, Aladdin), ethyl-4-chloro-3-hydroxybutyrate (98%, J&K Chemical Co., Ltd.), ethyl 4-bromoacetoacetate **26** (98%, J&K Chemical Co., Ltd.), ethyl (*S*)-4-bromo-3-hydroxybutyrate (98%, J&K Chemical Co., Ltd.), ethyl 4-bromo-3-hydroxybutyrate (98%, Donggang Pharmaceutical Co., Ltd., China), ethyl 4,4,4-trifluoro-3-oxobutanoate **27** (98%, Aldrich), ethyl (*S*)-4,4,4-trifluoro-3-hydroxyl butyrate (98%, Donggang Pharmaceutical Co., Ltd., China), ethyl 4,4,4-trifluoro-3-hydroxyl butyrate (98%, J&K Chemical Co., Ltd.), ethyl 4-phenyl-3-

oxopropanoate **28** (98%, J&K Chemical Co., Ltd.), ethyl (*S*)-4-phenyl-3-hydroxybutyrate (98%, Donggang Pharmaceutical Co., Ltd., China), ethyl 4-phenyl-3-hydroxybutyrate (98%, Donggang Pharmaceutical Co., Ltd., China), *t*-butyl 6-cyano-(*5R*)-hydroxyl-3-oxo hexanoate **30** (95%, Donggang Pharmaceutical Co., Ltd., China), *t*-butyl 6-cyano-(*3R*, *5R*)-dihydroxyl-hexanoate (95%, Donggang Pharmaceutical Co., Ltd., China), *t*-butyl 6-cyano-(*3S*, *5R*)-dihydroxyl-hexanoate (95%, Donggang Pharmaceutical Co., Ltd., China), *t*-butyl 6-chloro-(*5S*)-hydroxyl-3-oxo hexanoate **31** (90%, Donggang Pharmaceutical Co., Ltd., China), *t*-butyl 6-chloro-(*3R*, *5S*)-dihydroxyl hexanoate (90%, Donggang Pharmaceutical Co., Ltd., China), *t*-butyl 6-chloro-(*3S*, *5S*)-dihydroxyl hexanoate (90%, Donggang Pharmaceutical Co., Ltd., China), 5-((*4S*)-2-oxo-4-phenyl(1,3-oxazolidin-3-yl))-1-(4-fluoro phenyl)pentane-1,5-dione **32** (95%, Donggang Pharmaceutical Co., Ltd., China), (*4S*)-3-[(*5S*)-5-(4-fluorophenyl)-5-hydroxylpentanoyl]-4-phenyl-1,3-oxazolidin-2-one (95%, Dong gang Pharmaceutical Co., Ltd., China), (*4S*)-3-[5-(4-fluorophenyl)-5-hydroxy pentanoyl]-4-phenyl-1,3-oxazolidin-2-one (95%, Donggang Pharmaceutical Co., Ltd., China), (*E*)-2-[3-[3-[2-(7-chloro-2-quinolinyl)ethenyl]phenyl]-3-oxopropyl]benzoate **33** (95%, Donggang Pharma ceutical Co., Ltd., China), N,N-dimethyl-3-keto-3-(2-thienyl)-1- propanamine **34** (97%, Donggang Pharmaceutical Co., Ltd., China), (*S*)-N,N-dimethyl-3- hydroxy-3-(2-thienyl)-1-propanamine (98%, J&K Chemical Co., Ltd.), N,N-dimethyl-3-hydroxy-3-(2-thienyl)-1-propanamine (98%, J&K Chemical Co., Ltd.), sodium borohydride (99%, Aldrich), acetic acid (99%, Aldrich), dimethyl sulfoxide (DMSO) (99%, Aldrich), dimethylformamide (DMF) (99%, Aldrich), methanol (HPLC grade, Fisher), ethanol (HPLC grade, Fisher), acetone (99%, Aldrich), iso-propanol (HPLC grade, Fisher), n-butanol (99%, Aldrich), iso-butanol (99%, Aldrich),

tetrahydrofuran (THF) (99%, Aldrich), ethyl acetate (99%, Aldrich), butyl acetate (99%, Aldrich), iso-butyl acetate (99%, Aldrich), dichloromethane (99%, Aldrich), toluene (99%, Aldrich), xylene (99%, Aldrich), cyclohexane (98%, Aldrich), *n*-hexane (HPLC grade, Fisher), *n*-heptane (HPLC grade, Fisher), and *iso*-octane (99%, Aldrich).

The *Cp*SCR (GeneBank: GQ411433.1) was cloned from *Candida parapsilosis* previously discribed.[2] The glucose dehydrogenase (GDH) was obtained from *Exiguobacterium sibiricum* 255-15 (GenBank: ACB59697.1).[2b] The plasmid pMD18-T (Takara, Otsu, Japan) and strain *E. coli* JM109 (Tiangen biotech Co., Ltd., Beijing, China) were used for cloning. The plasmid pET28a (+) (Novagen, Darmstadt, Germany) and strain *E. coli* BL21 (DE3) (Invitrogen, Karlsruhe, Germany) were chosen for recombinant expression.

NAD(P)H and $NADP^+$ (sodium salt; >97% pure) were obtained from Roche (Karlsruhe, Germany). T4 DNA ligase, restriction enzymes, and PrimeSTAR® HS DNA polymerase were purchased from TaKaRa (Otsu, Japan). The *Pfu* DNA polymerase and *Taq* DNA polymerase were obtained from Biocolor (Shanghai, China). Antibiotics ampicillin (99%), kanamycin (99%) and IPTG (inducer, >99%) were purchased from Sigma Aldrich. Genomic DNA was extracted from strain *B. gladioli* ZJB12126 using a FastDNA® Spin Kit for Soil (MPBio, Shanghai, China). The DNA fragments were amplified through polymerase chain reaction (PCR) on Thermocycler (Bio-Rad, Hercules, CA, USA). Plasmid isolation, gel extraction, and PCR purification (Axygen Scientific, Inc, USA) were performed according to the manufactures' instructions. All of the PCR constructs were verified through DNA sequencing (Applied Biosystems, Foster, CA, USA). Plasmids DNA were transformed into *E. coli* through heat shock method.[3]

^{1}H and ^{13}C NMR spectra were recorded on a Bruker AVANCE III (1H NMR 500 MHz, 13C NMR 126 MHz). Absorption measurements were performed on a SpectraMax M5 microplate reader (Molecular Devices, CA) at 340 nm.

2. Identification of strain ZJB12126

Strain ZJB12126 was isolated from soil samples and exhibited active to convert BMOB to (*2S, 3R*)-MBHB (>80% *ee*, >80% *de*). It was taxonomically characterized and identified using morphological, physiological, and biochemical tests. The carbon source utilization and the chemical substrates sensitivity were determined by a standardized micromethod employing the Biolog microstation (see Table S1 and Table S2). The phylogenetic tree based on 16S rDNA sequence of ZJB12126 (1525 bp) was constructed by the neighbor-joining method. As shown in Figure S1, it was closely clustered with *Burkholderia gladioli* BSR3 (GenBank accession no. NR_102847.1) and showed 99% sequence identity. Thus, it was identified as *B. gladioli* ZJB12126 and deposited in China Center for Type Culture Collection (CCTCC No: M 2012379) for further studies.

Table S1. Sensitivity of 23 chemical-substrates by ZJB12126 using Biolog GEN III Microplate.

NO.	chemical-substrate	ZJB12126	NO.	chemical-substrate	ZJB12126
0	Positive Control	+	12	Lincomycin	+
1	pH 6	+	13	Guanidine HCl	−
2	pH 5	+	14	Niaproof 4	+
3	1% NaCl	+	15	Vancomycin	+
4	4% NaCl	−	16	Tetrazolium Violet	+
5	8% NaCl	−	17	Tetrazolium Blue	+
6	1% Sodium Lactate	+	18	Nalidixic Acid	−
7	Fusidic Acid	+	19	Lithium Chloride	−
8	D-Serine	−	20	Potassium Tellurite	−
9	Troleandomycin	+	21	Aztreonam	−
10	Rifamycin SV	+	22	Sodium Butyrate	−
11	Minocycline	−	23	Sodium Bromate	−

Notes: +, positive; −, negative; B, borderline

Table S2. Utilization of 71 carbon-substrates by ZJB12126 using Biolog GEN III Microplate.

NO.	carbon-substrate	ZJB12126	NO.	carbon-substrate	ZJB12126
0	Negative Control	−	36	Gelatin	−
1	Dextrin	−	37	Glycyl-L-Prolin	−
2	D-Maltose	−	38	L-Alanine	+
3	D-Trehalose	+	39	L-Arginine	+
4	D-Cellobiose	−	40	L-Aspartic	+
5	Gentiobiose	+	41	L-Glutamic Acid	+
6	Sucrose	−	42	L-Histidine	+
7	D-Turanose	−	43	L-Pyroglutamic Acid	+
8	Stachyose	−	44	L-Serine	+
9	D-Raffinose	−	45	Pectin	−
10	α-D-Lactose	−	46	D-Galacturonic Acid	−
11	D-Melibiose	−	47	L-Galactonic Acid Lactone	−
12	β-Methyl-D-Glucoside	−	48	D-Gluconic Acid	+
13	D-Salicin	−	49	D-Glucuronic Acid	B
14	N-Acetyl-D-Glucosamine	+	50	Glucuronamide	+
15	N-Acetyl-β-D-Mannosamine	−	51	Mucic Acid	+
16	N-Acetyl-D-Galactosamine	+	52	Quinic Acid	+
17	N-Acetyl Neuraminic Acid	−	53	D-Saccharic Acid	+
18	α-D-Glucose	+	54	p-Hydroxy-Phenylacetic Acid	−
19	D-Mannose	+	55	Methyl Pyruvate	+
20	D-Fructose	+	56	D-Lactic Acid Methyl Ester	−
21	D-Galactose	+	57	L-Lactic Acid	+
22	3-Methyl Glucose	−	58	Citric Acid	+
23	D-Fucose	+	59	α-Keto-Glutaric Acid	−
24	L-Fucose	+	60	D-Malic Acid	+
25	L-Rhamnose	−	61	L-Malic Acid	+
26	Inosine	+	62	Bromo-Succinic Acid	B
27	D-Sorbitol	+	63	Tween 40	+
28	D-Mannitol	+	64	γ-Amino-Butryric Acid	+
29	D-Arabitol	+	65	α-Hydroxy-Butyric Acid	+
30	myo-Inositol	+	66	β-Hydroxy-D,L Butyric Acid	+
31	Glycerol	+	67	α-Keto-Butyric Acid	+
32	D-Glucose-6-PO_4	+	68	Acetoacetic Acid	B
33	D-Fructose-6-PO_4	+	69	Propionic Acid	+
34	D-Aspartic Acid	+	70	Acetic Acid	+
35	D-Serine	+	71	Formic Acid	+

Notes: +, positive; −, negative; B, borderline

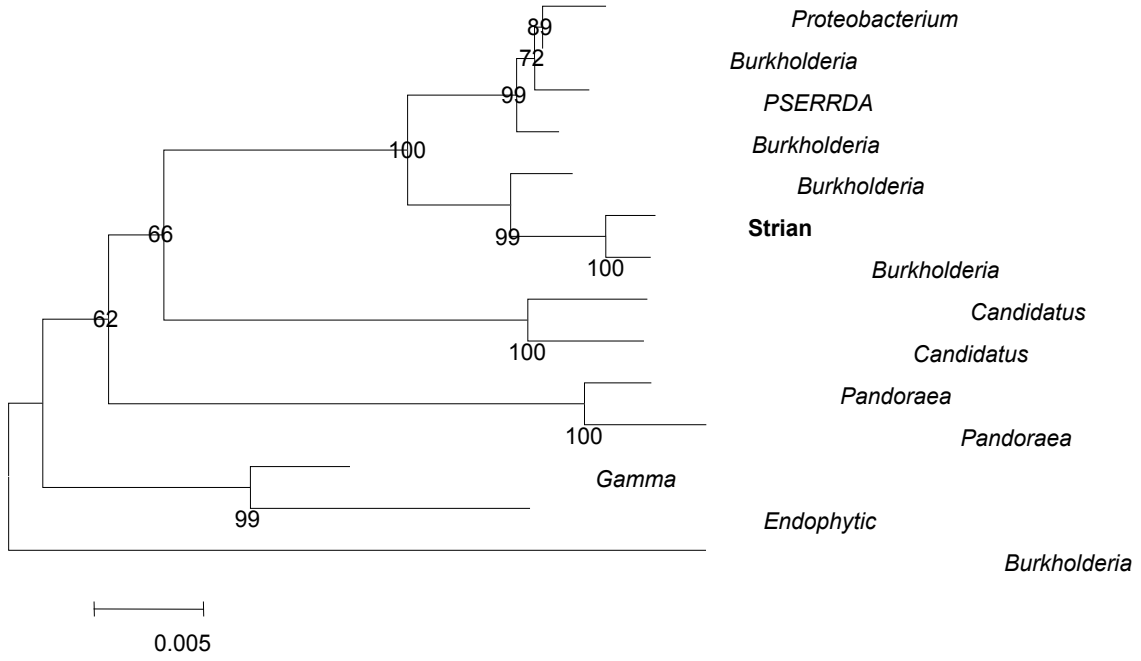

Figure S1. The phylogenetic tree based on 16S rDNA, constructed by the neighbor-joining method, showing the relationship between strain ZJB12126 and representatives of some related taxa. *Numbers in parentheses* are accession numbers of published sequences. Bootstrap values (1,000 replications) are shown as percentages at branch points.

3. Preparation of recombinant enzymes

The *bgadh* genes were amplified from the genomic DNA of *B. gladioli* ZJB12126 using primers listed in Table S3. The target products were inserted into pMD18-T, and digested with restriction endonucleases (*Xba* I and *Xho* I for *Bg*ADH1, *Nco* I and *Xho* I for *Bg*ADH2 and *Bg*ADH5). Then, the fragments were ligated with pET28a (+) and transformed into *E. coli* BL21 (DE3). Single colonies were cultured in LB/Kanamycin (50 μg mL^{-1}) at 37 °C and 150 rpm until OD_{600} was between 0.6 and 0.8, and induced with IPTG (0.1 mM) at 28 °C for 8 h. Since the recombinant enzymes were expressed as His_6-tagged proteins in *E. coli*, one-step purification was adopted on metal chelate affinity chromatography.[4] The protein expression

and purification were checked on sodium dodecyl sulfatepolyacrylamide gel electrophoresis (SDS-PAGE) (Figure S2). The molecular mass of the native enzymes were determined on a Discovery BIO GFC 150 (300 × 7.8 mm, 3 μm) column (Sigma-Aldrich, USA) equilibrated in 150 mM phosphate (pH 7.0). Protein concentrations were determined using Bradford reagents (Bio-Rad) with bovine serum albumin (BSA) as a standard. Purified enzymes were used in all of the experiments in this study.

Table S3. Primers for PCR amplification.

Primers	Oligonucleotide sequences
*Bg*ADH1	*Bg*ADH1-F: 5'-tctagaATGGGTCGTTCGATCAATCTGGAAGG-3'
	*Bg*ADH1-R: 5'-ctcgagTGCGAGCCCGAATCCGTCGTCG-3'
*Bg*ADH2	*Bg*ADH2-F: 5'-ccatggGCAAGCGGCTGGAAGGCAAGG-3'
	*Bg*ADH2-R: 5'-ctcgagGACCTGGGCCTGGCCGCCG-3'
*Bg*ADH5	*Bg*ADH5-F: 5'-ccatggCAGACGTCAACAGCCTGTTC-3'
	*Bg*ADH5-R: 5'-ctcgagGACCGTGCTGGTGAGGCC-3'

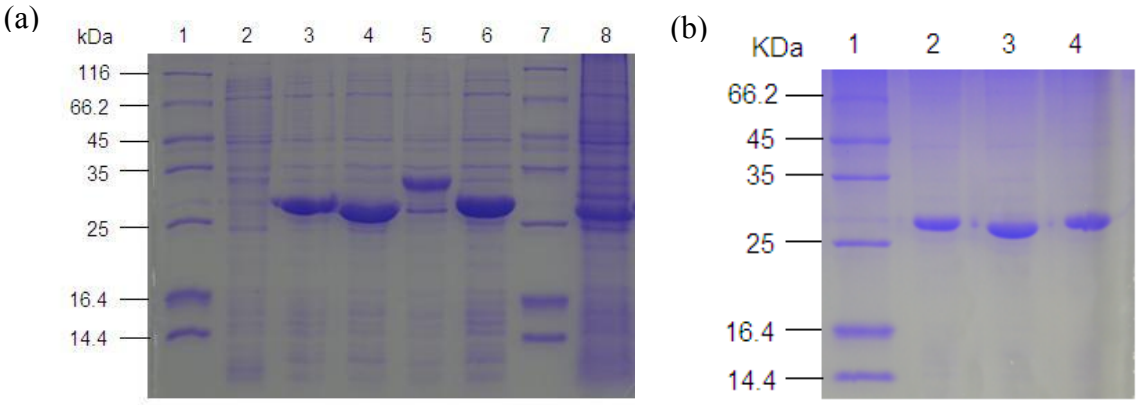

Figure S2. (a) The SDS-PAGE analysis of the overexpression of *Bg*ADHs and *Cp*SCR. The proteins were separated on a 12% SDS-polyacrylamide gel and stained with Coomassie Brilliant Blue G-250. Lane 1, molecular mass standard; Lane 2, *E. coli* BL21(DE3)/pET28a; Lane 3, *Bg*ADH1; Lane 4, condon optimized *Bg*ADH2; Lane 5, *Cp*SCR; Lane 6, *Bg*ADH5; Lane 7, molecular mass standard; Lane 8, unoptimized *Bg*ADH2. (b) The SDS-PAGE analysis of purified *Bg*ADHs. Lane 1, molecular weight mark; Lane 2, the purified *Bg*ADH1; Lane 3, the purified *Bg*ADH2; Lane 4, the purified *Bg*ADH5.

In order to improve the expression level of *Bg*ADH2, condon optimization was adopted according to the codon bias in *E. coli* (http://www.kazusa.or.jp/codon/), in which Arg codons (AGA, CGA), Leu codon (CUA), Ile codon (AUA), Gly codon (GGA), and Pro codon (CCC) are considered as the rare codons.[5] The codon optimized *Bg*ADH2 was designed and five rare codons were replaced with the synonymous ones used at the highest frequency, in detail, two CGGs, GGG/CCC, and ACT were substituted for CGCs, GGC/CCG, and ACC, respectively. The pET28a-*bgadh2* was employed as the template and one-step mutagenesis reaction protocol was performed using PrimeSTAR® HS DNA polymerase. The oligonucleotide primers (with mutation codon underlined) are summarized in Table S4. The result was shown in Figure S2.

Table S4. Primers designed for the codon optimization and site-directed mutagensis of *Bg*ADH2.

Primers	Oligonucleotide sequences
*Bg*ADH2-F4	5'-GGCAGCCATATGGGCAAGCGCCTGGAAGGCAAGGTGGCA-3'
*Bg*ADH2-R4	5'-TGCCACCTTGCCTTCCAGGCGCTTGCCCATATGGCTGCC-3'
*Bg*ADH2-F18	5'-GTAACGGGCGGCACGAGCGGGATCGGCCTGGCCACCGCG-3'
*Bg*ADH2-R18	5'- CGCGGTGGCCAGGCCGATCCCGCTCGTGCCGCCCGTTAC-3'
*Bg*ADH2-F81	5'-ATCCGCGCCACCGAAGGCCGCCTCGACGTGCTGTTCACC-3'
*Bg*ADH2-R81	5'-GGTGAACAGCACGTCGAGGCGGCCTTCGGTGGCGCGGAT-3'
*Bg*ADH2-F119	5'-GTGAAGGCGGTGGTGTTCACCGTGCAGAAGGCCCTGCCG-3'
*Bg*ADH2-R119	5'-CGGCAGGGCCTTCTGCACGGTGAACACCACCGCCTTCAC-3'
*Bg*ADH2-F180	5'-CGCGTCAACGTGGTGAGCCCGGGCTCGACGCGCACCATC-3'
*Bg*ADH2-R180	5'-GATGGTGCGCGTCGAGCCCGGGCTCACCACGTTGACGCG-3'
S138A-F	5'-GATCATCCTGAACGGCGCGATCGCGGGCTCGACG-3'
S138A-R	5'-CGTCGAGCCCGCGATCGCGCCGTTCAGGATGATC-3'
Y151A-F	5'-CAGGCCTTCAGCATCGCGGGCGCCTCGAAGGCCG-3'
Y151A-R	5'-CGGCCTTCGAGGCGCCCGCGATGCTGAAGGCCTG-3'

To support the speculated statements about the molecular basis of *Bg*ADH2 toward BMOB, site-directed mutagenesis was adopted using one-step mutagenesis reaction protocol as well. The oligonucleotide primers (with mutation codon underlined) are also summarized in Table S4.

4. Sequence alignment of *Bg*ADHs with several known alcohol dehydrogenases

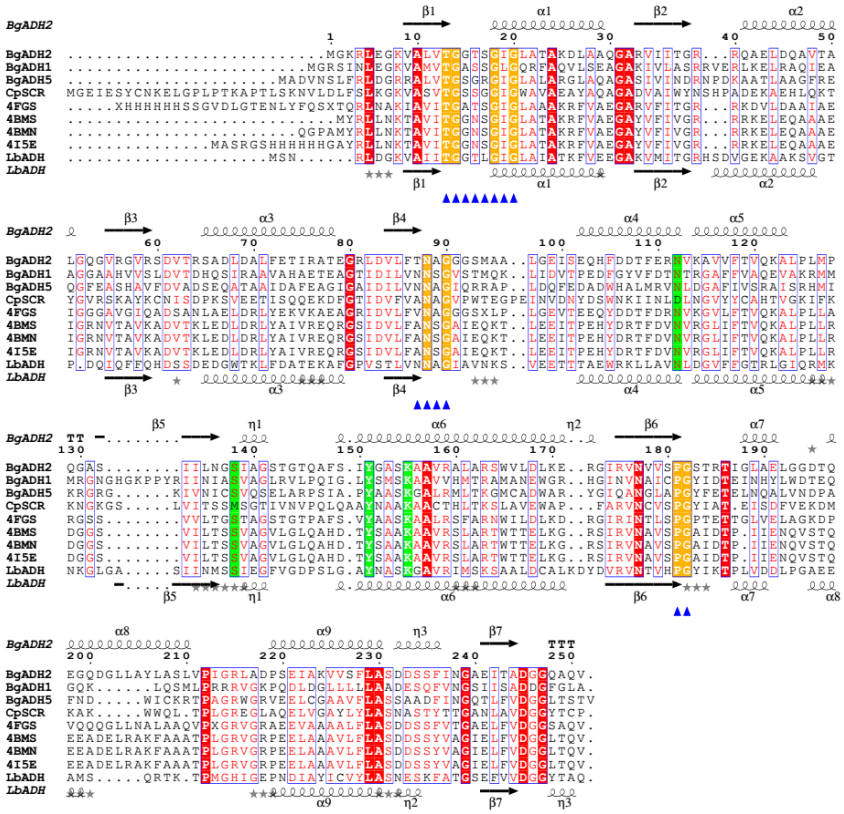

Figure S3. Multiple sequence alignments of *Lb*ADH from *Lactobacillus brevis* (GeneBank: CAD66648.1), *Cp*SCR from *Candida parapsilosis* (GeneBank: GQ411433.1), *Rhizobium etli* alcohol dehydrogenase (PDB: 4FGS), *Ralstonia* sp. alcohol dehydrogenases (PDB: 4BMS, 4BMN, and 4I5E), *Bg*ADH1 (GeneBank: YP_004360366.1), *Bg*ADH2 (GeneBank: YP_004348055.1), and *Bg*ADH5 (GeneBank: YP_004349253.1). The cofactor-binding motifs in the SDRs, TGXXXGXG, NNAG, and PG, are highlighted in orange and triangle while the residues of the catalytic tetrad (N, S, Y, and K) are highlighted in green.

5. Enzyme assay

Specific activities were assayed spectrophotometrically by observing the depletion of NAD(P)H at 340 nm. One unit of enzyme activity was defined as 1 μmol of NAD(P)H

consumed per minute under the assay conditions. Each assay contained substrate (40 mM) and NAD(P)H (0.4 mM). Hydrophobic substrates were dissolved in DMSO prior to dilution into buffer to give a final DMSO concentration of 5% (v/v). Unless otherwise stated, phosphate buffer (100 mM, pH 6.5) was used. Blank reading of the non-specific decomposition of NAD(P)H was use as the appropriate correction.

6. Synthesis of methyl 2-benzamido-methyl-3-oxobutyrate (BMOB) 29

N-(chloromethyl)benzamide: To a mixture of N-(hydroxymethyl)benzamide (15.1 g, 0.1 mol) and dried ether solution (40 mL) cooled at -5 °C, phosphorus pentachloride (20.8 g, 0.1 mol) was slowly added with stirring. The addition rate of phosphorus pentachloride was maintained in such a way that the reaction temperature does not exceed 5 °C and the addition time was about 1 h. Upon complete addition, the reaction temperature was raised to ambient temperature and stirred for further 1.5 h. The product was collected by filtration and used for the next synthetic step without further purification (14.5 g, 85%).

Methyl 2-benzamido-methyl-3-oxobutanoate (BMOB): A DMF solution of (Z)-methyl 3-(pyrrolidin-1-yl)but-2-enoate (14.5 g, 0.085 mol) was cooled at 0 °C followed by the slowly addition of N-(chloromethyl)benzamide (14.5 g, 0.085 mol) with stirring. After complete addition, the reaction temperature was raised to 30 °C for additional 1 h. The reaction mixture was transferred in water (200 mL) and the precipitation was filtrated. The crude product was purified by flash chromatography on a silica gel conlumn (ethyl acetate/petroleum ether = 3:1, R_f = 0.5), affording 15 g (71%) of BMOB as white powder. ^{1}H NMR (500 MHz, DMSO-d_6): δ=8.63 (m, NH-1H), 7.81 (m, Ph-2,6-2H), 7.52 (m, Ph-3,4,5-3H), 4.01 (t, *J*=7.1 Hz, C-2-1H),

3.70 (m, OCH_3-3H, N-CH_2-2H), and 2.24 (s, C-4-3H). ^{13}C NMR (126 MHz, DMSO-d_6): δ=202.10 (s, C-3), 168.63 (s, C-COO), 166.63 (s, C-CONH), 134.02 (s, C-Ph-1), 131.28 (s, C-Ph-4), 128.26 (s, C-Ph-3,5), 127.14 (s, C-Ph-2,6), 58.10 (s, C-2), 52.33 (s, C-OCH_3), 37.88 (d, *J*=21.0 Hz, C-CH_2), and 29.27 (s, C-4).

7. Synthesis of methyl-2-benzamido-methyl-3-hydroxy-butyrate (MBHB)

Methyl-2-benzamido-methyl-3-hydroxy-butyrate (MBHB) was obtained by non-stereoselective reduction with sodium borohydride ($NaBH_4$) from BMOB: A methanol solution of BMOB (15 g, 0.06 mol) in dried three-neck flask (250 mL) was cooled to 0 °C and sodium borohydride (0.95 g, 0.025 mol) was slowly added with stirring. Then, the reaction temperature was raised to room temperature for 2 h. After complete reaction, the pH of reaction mixture was adjusted to 5-6 with 10% acetic acid/methanol solution and the mixture was extracted twice with ethyl acetate. The organic phase was separated, dried over Na_2SO_4 and removed by evaporation. The crude product was purified by flash chromatography on a silica gel conlumn (ethyl acetate/petroleum ether = 3:1, R_f = 0.28 and 0.32), offering 10 g (66.7%) of MBHB as oily liquid. ^1H NMR (500 MHz, DMSO-d_6): δ=8.51 (t, *J*=5.5 Hz, NH-1H), 7.80 (m, Ph-2,6-2H), 7.52 (m, Ph-4-1H), 7.46 (m, Ph-3,5-2H), 4.88 (d, *J*=5.5 Hz, C-3-1H), 3.85 (dd, *J*=12.3 Hz, C-2-1H), 3.58 (s, OCH_3-3H), 3.45 (m, N-CH_2-2H), 2.72 (dt, *J*=8.4 Hz, OH-1H), and 1.16 (d, *J*=6.3 Hz, C-4-3H). ^{13}C NMR (126 MHz, DMSO-d_6): δ=172.88 (s, C-COO), 166.46 (s, C-CONH), 134.43 (s, C-Ph-1), 131.11 (s, C-Ph-4), 128.23 (s, C-Ph-3,5), 127.13 (s, C-Ph-2,6), 65.83 (s, C-2), 52.98 (s, C-3), 51.19 (s, C-OCH_3), 38.44 (m, C-CH_2), and 21.29 (s, C-4).

The four isomers of MBHB were collected using semi-preparative HPLC in our laboratory. The purities of (*2S, 3R*)-MBHB, (*2R, 3R*)-MBHB, (*2R, 3S*)-MBHB and (*2S, 3S*)-MBHB were 97.8%, 96.7%, 96.9%, and 96.4%, respectively. [6]

8. Screening of recombinant *Bg*ADHs for DYKAT of BMOB

Each reaction mixture was comprised of phosphate buffer (100 mM, pH 6.5), BMOB **29** (40 mM, DMSO, 5% v/v), $NADP^+$ (0.4 mM), glucose (5%, w/v), GDH (0.1 mg mL^{-1}), and purified enzyme (0.1 mg mL^{-1}) in a total volumn of 1 mL. The reaction proceeded at 30 ^oC for 16 h. Reaction mixture without recombinant enzyme was used as the control. Aliquot of biotransformation solution (100 μL) was withdrawn, extracted twice with ethyl acetate (200 μL), and analyzed by HPLC.

9. Characterization of *Bg*ADHs

Optimal pH. Since the environmental pH affect the enzymatic activity, different pH values were tested in disodium hydrogen phosphate-citrate (100 mM, pH 3.5, 4.0, 4.5, 5.0, 5.5, 6.0, 6.5, and 7.0), potassium phosphate (100 mM, pH 6.0, 6.5, 7.0, 7.5, and 8.0), Tris-HCl buffer (100 mM, pH 7.5, 8.0, 8.5, and 9.0), and Gly-NaOH buffer (100 mM, pH 9.0, 9.5, 10.0, and 10.5). The results were listed in Figure S4-S6.

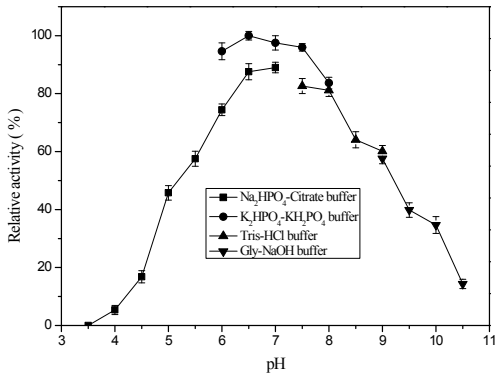

Figure S4. Effect of pH on the specific activity of the purified *Bg*ADH1.

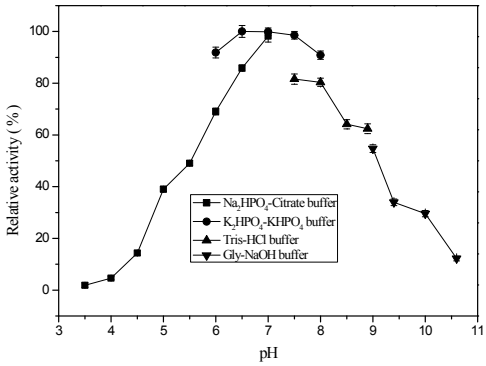

Figure S5. Effect of pH on the specific activity of the purified *Bg*ADH2.

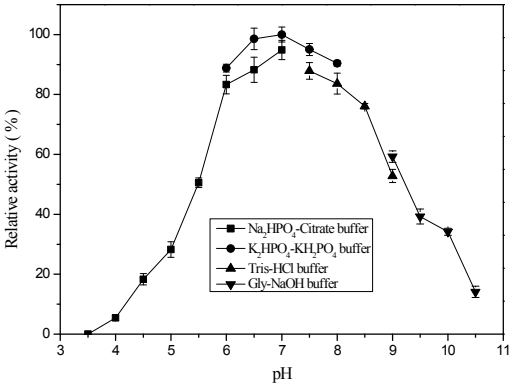

Figure S6. Effect of pH on the specific activity of the purified *Bg*ADH5.

Optimal temperature and thermostabiliy. The optimal temperatures of *Bg*ADHs were studied by assaying enzyme activities at temperatures ranging from 25 ^{o}C to 65 ^{o}C in phosphate

buffer (100 mM, pH 6.5). To evaluate the thermostability of *Bg*ADHs, purified enzymes were diluted to 0.5 mg mL^{-1} in phosphate buffer (100 mM, pH 6.5) and incubated at temperatures ranging from 4 °C to 65 °C. Samples were withdrawn per hour and the residual activities were detected under the standard condition. The results were shown in Figure S7-S9.

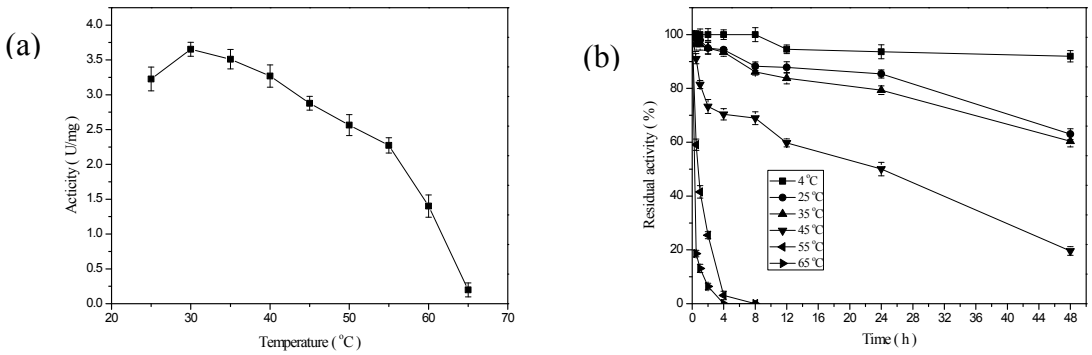

Figure S7. Effect of temperature on the specific activity (a) and stability (b) of the purified *Bg*ADH1.

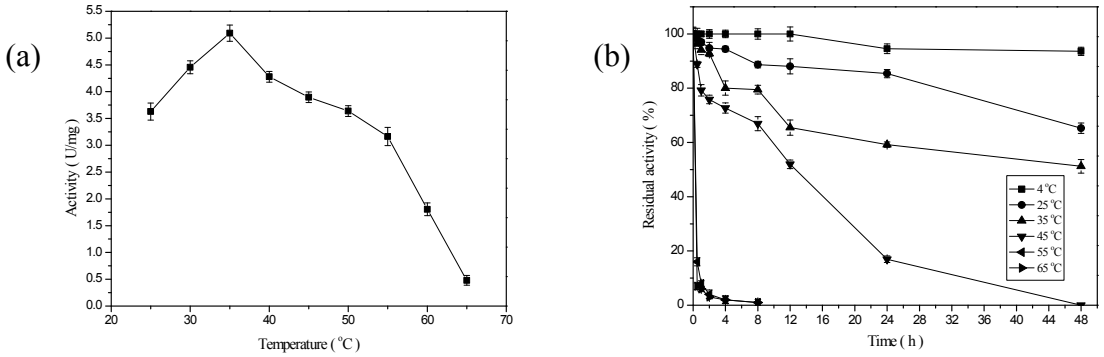

Figure S8. Effect of temperature on the specific activity (a) and stability (b) of the purified *Bg*ADH2.

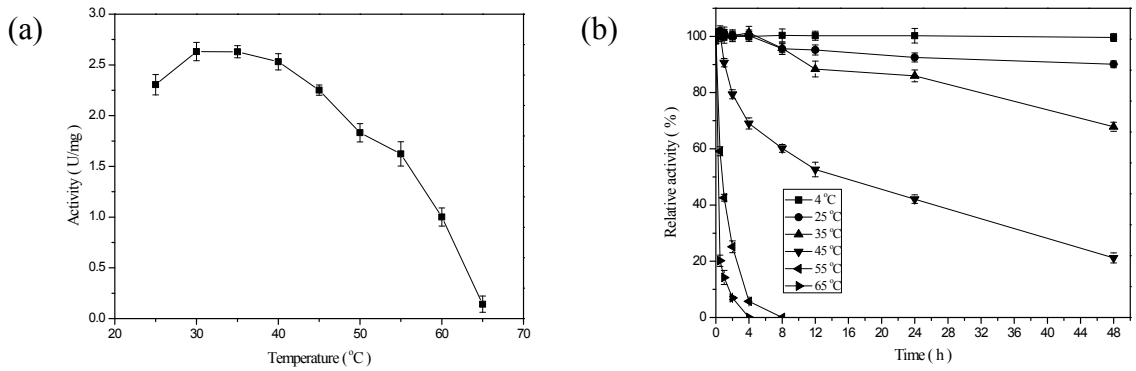

Figure S9. Effect of temperature on the specific activity (a) and stability (b) of the purified *Bg*ADH5.

Effects of metal ions and chemical additives. To investigate the effects of metal ions and chemical additives on the activities of *Bg*ADHs, the initial activities were tested at 30 °C in the presence of various metal ions (Fe^{2+}, Ni^{2+}, Cu^{+}, Fe^{3+}, Ca^{2+}, Ba^{2+}, Cu^{2+}, Mn^{2+}, Zn^{2+}, Co^{2+}, Mg^{2+}, Ag^{+}, and Hg^{2+}), EDTA-Na_2, Triton-X100, and Tween 80 (2 mM). The result was summarized in Table S5.

Kinetic parameters. All assays were carried out at 30 °C, and, unless otherwise stated, in phosphate buffer (100 mM, pH 6.5). Using BMOB as the substrate, multiple measurements were done under conditions where BMOB was held at constant concentration (40 mM) and NADH or NADPH concentrations varied from 0.04 to 1.6 mM or 0.01 to 0.4 mM. Additionally, multiple experiments with different BMOB concentrations ranged from 0.04 to 40 mM were performed in the presence of constant NADPH (0.4 mM). The kinetic parameters were calculated by nonlinear regression to the Michaelis-Menten equation aided by Origin software (OriginLab Corporation, Northampton, MA). Unless otherwise stated, estimation errors of kinetic parameters were <20%. The result was listed in Table S6.

Table S5. Effect of metal ions and chemical agents on the activities of *Bg*ADHs.[a]

Reagent	Concentration	Relative activity (%)		
		*Bg*ADH1	*Bg*ADH2	*Bg*ADH5
Control	-	100±2.5	100±2.1	100±2.5
Fe^{2+}	2 mM	86±3.7	68±1.5	98±1.6
Ni^{2+}	2 mM	72±1.5	60±3.2	100±2.1
Cu^{+}	2 mM	25±2.1	21±1.9	37±0.9
Fe^{3+}	2 mM	55±0.9	13±1.5	81±0.6

Ca^{2+}	2 mM	76±2.1	80±6.2	95±1.5
Ba^{2+}	2 mM	85±2.4	70±5.3	97±2.6
Cu^{2+}	2 mM	63±3.2	14±2.2	93±2.4
Mn^{2+}	2 mM	55±2.0	55±2.3	81±3.1
Zn^{2+}	2 mM	120±2.6	139±5.2	98±3.6
Co^{2+}	2 mM	30±1.9	11±1.2	39±2.0
Mg^{2+}	2 mM	124±5.5	128±2.7	98±3.1
Ag^{+}	2 mM	27±1.5	17±1.2	29±1.5
Hg^{2+}	2 mM	5±0.6	2±0.1	7±0.9
EDTA-Na_2	2 mM	102±2.4	105±3.2	99±1.8
Triton-X100	2 mM	100±2.6	105±3.8	97±2.5
Tween 80	2 mM	106±6.9	110±2.5	99±2.3

[a] Enzyme activities were determined under standard assay conditions after incubation with metal ions and chemical agents at 30 °C for 30 min. The activity in the absence of metal ions and chemical agents was recorded as 100%.

Table S6. Kinetic parameters for the DYKAT of BMOB by *Bg*ADH1, *Bg*ADH2, *Bg*ADH5, and *Cp*SCR.

Enzyme	K_m (mM)		$k_{cat\ BMOB}$ (s^{-1})	$k_{cat}/K_{m\ BMOB}$ ($s^{-1}\cdot mM^{-1}$)
	NAD(P)H	BMOB		
*Bg*ADH1[a]	0.083	1.47	8.57	5.83
*Bg*ADH1[b]	0.234	-	-	-
*Bg*ADH2[a]	0.043	2.30	29.9	12.3
*Bg*ADH2[b]	0.96	-	-	-
*Bg*ADH5[a]	0.13	3.37	9.47	2.81
*Bg*ADH5[b]	0.61	-	-	-
*Cp*SCR[a]	-	2.22	22.2	10.0

[a] NADPH. [b] NADH. Reaction conditions: BMOB (40 mM, DMSO, 5% v/v), purified enzyme (0.1 mg mL^{-1}), NADH (0.04 to 1.6 mM) or NADPH (0.01 to 0.4 mM), pH 6.5, and 30 °C toward NAD(P)H; BMOB (0.04 to 40 mM, DMSO, 5% v/v), enzyme (0.1 mg mL^{-1}), NADPH (0.4 mM), pH 6.5, and 30 °C toward BMOB.

10. Effect of organic solvents on asymmetric synthesis of (*2S, 3R*)-MBHB using *Bg*ADH2

The influence of organic solvents on the activity of *Bg*ADH2 was assessed using BMOB as substrate under the enzyme assay protocol in the presence of water-miscible (25%, v/v, dimethyl sulfoxide, dimethylformamide, methanol, ethanol, acetone, *iso*-propanol, *n*-butanol, and *iso*-butanol) and water-immiscible solvents (50%, v/v, tetrahydrofuran, ethyl acetate, butyl acetate, iso-butyl acetate, dichloromethane, toluene, xylene, cyclohexane, *n*-hexane, *n*-heptane,

and *iso*-octane). The effect of organic solvents on the stereo-selectivity of *Bg*ADH2 in the asymmetric synthesis of (*2S, 3R*)-MBHB was investigated by adding BMOB (40 mM, DMSO, 5% v/v), glucose (5%, w/v), $NADP^+$ (0.4 mM), purified *Bg*ADH2 (0.1 mg mL^{-1}), and GDH (0.1 mg mL^{-1}) at 35 ^oC for 8 h.

11. Asymmetric synthesis of (*2S, 3R*)-MBHB using *Bg*ADH2 in single aqueous system

Biotransformation reactions were performed with a certain concentration of BMOB (5-140 mM, DMSO, 10% v/v), glucose (5%, w/v), $NADP^+$ (0.4 mM), purified *Bg*ADH2 (0.1 mg mL^{-1}), and GDH (0.1 mg mL^{-1}) in 20 mL phosphate buffer (100 mM, pH 6.5) at 35 ^oC for 8 h. The residual was extracted twice with ethyl acetate, and analyzed by HPLC.

12. Asymmetric synthesis of (*2S, 3R*)-MBHB in aqueous-toluene biphasic system

Reactions were performed with a certain concentration of BMOB (5-140 mM, DMSO, 10% v/v), $NADP^+$ (0.4 mM), glucose (5%, w/v), purified *Bg*ADH2 (0.1 mg mL^{-1}), and GDH (0.1 mg mL^{-1}) in 10 mL phosphate buffer (100 mM, pH 6.5) mixed with an equal volume of toluene at 35 ^oC for 8 h. After reaction, the two layers were separated and the aqueous layer was extracted twice with ethyl acetate. The extracted layers were combined with the original organic layer, and subsequently analyzed by HPLC.

Time course of (*2S, 3R*)-MBHB production using *Bg*ADH2 was achieved by adding BMOB (60 mM, DMSO, 5% v/v), $NADP^+$ (0.4 mM), glucose (5%, w/v), purified *Bg*ADH2 (0.1 mg mL^{-1}), and GDH (0.1 mg mL^{-1}) in 10 mL phosphate buffer (100 mM, pH 6.5) mixed

with an equal volume of toluene at 35 °C for 8 h. Aliquot of mixture (100 μL) in the organic layer was removed at predetermined times and analyzed by HPLC. The conversion, *ee* and *de* values were calculated as previously described.[6] ^{1}H NMR (500 MHz, DMSO-d_6): δ=8.50 (t, *J*=5.5 Hz, NH-1H), 7.80 (m, Ph-2,6-2H), 7.52 (m, Ph-4-1H), 7.46 (m, Ph-3,5-2H), 4.99 (d, *J*=5.5 Hz, C-3-1H), 3.81 (dd, *J*=12.3 Hz, C-2-1H), 3.64 (s, OCH_3-3H), 3.34 (m, N-CH_2-2H), 2.67 (dt, *J*=8.4 Hz, OH-1H), and 1.10 (d, *J*=6.3 Hz, C-4-3H). ^{13}C NMR (126 MHz, DMSO-d_6): δ=172.83 (s, C-COO), 166.42 (s, C-CONH), 134.41 (s, C-Ph-1), 131.08 (s, C-Ph-4), 128.21 (s, C-Ph-3,5), 127.10 (s, C-Ph-2,6), 65.80 (s, C-2), 52.95 (s, C-3), 51.17 (s, C-OCH_3), 38.40 (m, C-CH_2), and 21.26 (s, C-4).

13. Substrate specificities of *Bg*ADHs

Each reaction mixture contained phosphate buffer (100 mM, pH 6.5), substrate (40 mM), $NADP^+$ (0.4 mM), glucose (5%, w/v), GDH (0.1 mg mL^{-1}), and purified enzyme (0.1 mg mL^{-1}) in a total volumn of 1 mL and proceeded at 30 °C for 16 h. Reaction mixture without recombinant enzyme was used as the control. Hydrophobic substrates were dissolved in DMSO prior to dilution into buffer to give a final DMSO concentration of 5% (v/v). After complete addition, biotransformation solution was extracted with ethyl acetate and analyzed by HPLC or GC. For substrates with hydrophilic groups (**20**, **21**, and **22**), the supernatant of reaction solution was detected directly by RP-HPLC.

14. Analytical methods

The *ee* or *de* values of products from biotransformation were determined using GC-14C (Shimadu, Japan), Model LC-20AT (Shimadu, Japan), or Dionex UltiMate 3000 (Dionex, USA). The analysis conditions and retention times of substrates and each isomer for the corresponding bioproducts were summaried in Table S7.

Table S7. GC and HPLC analysis of the *ee* or *de* values of chiral alcohols.

Product	Chiral column[a]	Conditions	Retention time (min)		
			substrate	(*S*)-P	(*R*)-P
P10	BGB-174	110 °C, 5 °C min^{-1}, 160 °C; Inc./dec. 240 °C; helium	6.7	7.6	7.9
P11	BGB-174	110 °C, 5 °C min^{-1}, 160 °C Inc./dec. 240 °C; helium	7.8	8.8	9.2
P12	OJ-H	*n*-hexane/isopropanol (97:3, v/v); flow rate: 0.2 mL min^{-1}; 254 nm	9.1	18.9	20.2
P13	OJ-H	*n*-hexane/isopropanol (97:3, v/v); flow rate: 0.2 mL min^{-1}; 254 nm	10.3	19.4	21.2
P14	OJ-H	*n*-hexane/isopropanol (97:3, v/v); flow rate: 0.2 mL min^{-1};254 nm	13.3	25.0	41.7
P15	BGB-174	140 °C; Inc./dec. 240 °C; helium	5.1	6.3	6.8
P16	BGB-174	140 °C; Inc./dec. 240 °C; helium	3.5	5.8	6.1
P17	BGB-174	140 °C; Inc./dec. 240 °C; helium	3.6	6.1	6.3
P18	OJ-H	*n*-hexane/isopropanol (95:5); flow rate: 0.2 mL min^{-1}; 254 nm	9.6	11.4	12.1
P20	Chirobiotic ™ R	0.5% AcOH-CH_3CN (20:80, v/v); flow rate of 1.0 mL/min; 278 nm	9.5	3.0	3.3
P21	Chirobiotic ™ R	0.5% AcOH-CH_3CN (20:80, v/v); flow rate of 1.0 mL/min; 215 nm	7.6	3.4	3.6
P22	Chirobiotic ™ R	0.5% AcOH-CH_3CN (20:80, v/v); flow rate of 1.0 mL/min; 215 nm	6.6	3.8	4.0
P23	BGB-174	110 °C, 20 min, 5 °C min^{-1}, 160 °C; Inc./dec. 240 °C; helium	10.8	24.4	23.9

Continued

Product	Chiral column[a]	Conditions	Retention time (min)		
			substrate	(*S*)-P	(*R*)-P
P24	BGB-174	110 °C, 20 min, 5 °C min^{-1}, 160 °C; Inc./dec. 240 °C; helium	6.2	19.3	18.9

P25	BGB-174	110 °C, 0.5 °C min^{-1}, 125 °C; Inc./dec. 240 °C; helium	7.1	25.0	24.7
P26	BGB-174	110 °C, 25 min, 5 °C min^{-1}, 160 °C, 2 min; Inc./dec. 240 °C; helium	9.3	34.6	34.4
P27	BGB-174	120 °C; Inc./dec. 240 °C; helium	3.8	7.2	6.8
P28	AD-H	*n*-hexane/isopropanol (95:5); flow rate: 1.0 mL min^{-1}; 218 nm	4.9	8.1	7.9
P29	AY-H	*n*-hexane/ethanol (76:24); flow rate: 1.0 mL min^{-1}; 254 nm	9.8, 11.0	5.8 for (*2S,3R*), 6.7 for (*2R,3R*)	7.3 for (*2R,3S*), 10.3 for (*2S,3S*)
P30	ODS	acetonitrile/water (1:3, v/v); flow rate: 1.0 mL min^{-1}; 220 nm	11.4	10.3	9.8
P31	ODS	acetonitrile/water (1:3, v/v); flow rate: 1.0 mL min^{-1}; 220 nm	16.4	14.2	13.8
P32	OD-H	*n*-hexane/ethanol (80:20, v/v); flow rate: 1.0 mL min^{-1}; 215 nm	22.0	19.7	17.2
P33	OD-H	*n*-hexane/isopropanol (80:20); flow rate: 1.0 mL min^{-1}; 287 nm	12.8	14.4	16.4
P34	OJ-H	*n*-heptane/ethanol/diethylamine(99:1:0.2, v/v); flow rate: 0.2 mL min^{-1}; 235 nm	7.3	8.9	10.1

[a] BGB-174 (30 m × 0.25 mm × 0.25 µm; BGB Analytik); Chiralcel OJ-H column (2.1 × 150 mm; Daicel Chemical Ind. Ltd., Japan); Chirobiotic ™ R (4.6 mm×250 mm, Sigma, USA); Chiralpak AD-H column (4.6 × 150 mm; Daicel Chemical Ind. Ltd., Japan); Hypersil ODS column (4.6 mm × 250 mm, Thermo, USA); Chiralpak AY-H column (4.6 × 250 mm; Daicel Chemical Ind. Ltd., Japan); Chiralcel OD-H column (4.6 × 250 mm; Daicel Chemical Ind. Ltd., Japan).

15. Homology modeling and docking

Searching for structures related to *Bg*ADH2 was performed using pBLAST (www.ncbi.nlm.nih.gov/blast) from Protein Data Bank Database and the most appropriate templates were selected according to the sequence similarity among the possible templates. Amino acid sequence alignments were created with software package Clustal X2 and the ESPript 3.0 network station.[7] The three-dimensional (3D) model of *Bg*ADH2 was constructed using MODELER 9.12 based on the crystal structures of *Rhizobium etli* alcohol dehydrogenase (PDB: 4FGS), *Ralstonia* sp. alcohol dehydrogenases (PDB: 4BMS, 4BMN, and 4I5E), by multi-template homology modeling (John Wiley & Sons Software, San Francisco, CA).[8] The

best quality model was evaluated by PROCHECK (EMBI-EBI, Cambridge, UK) and was chosen for further docking studies by Autodock 4.0.[9]

16. Chiral GC chromatograms

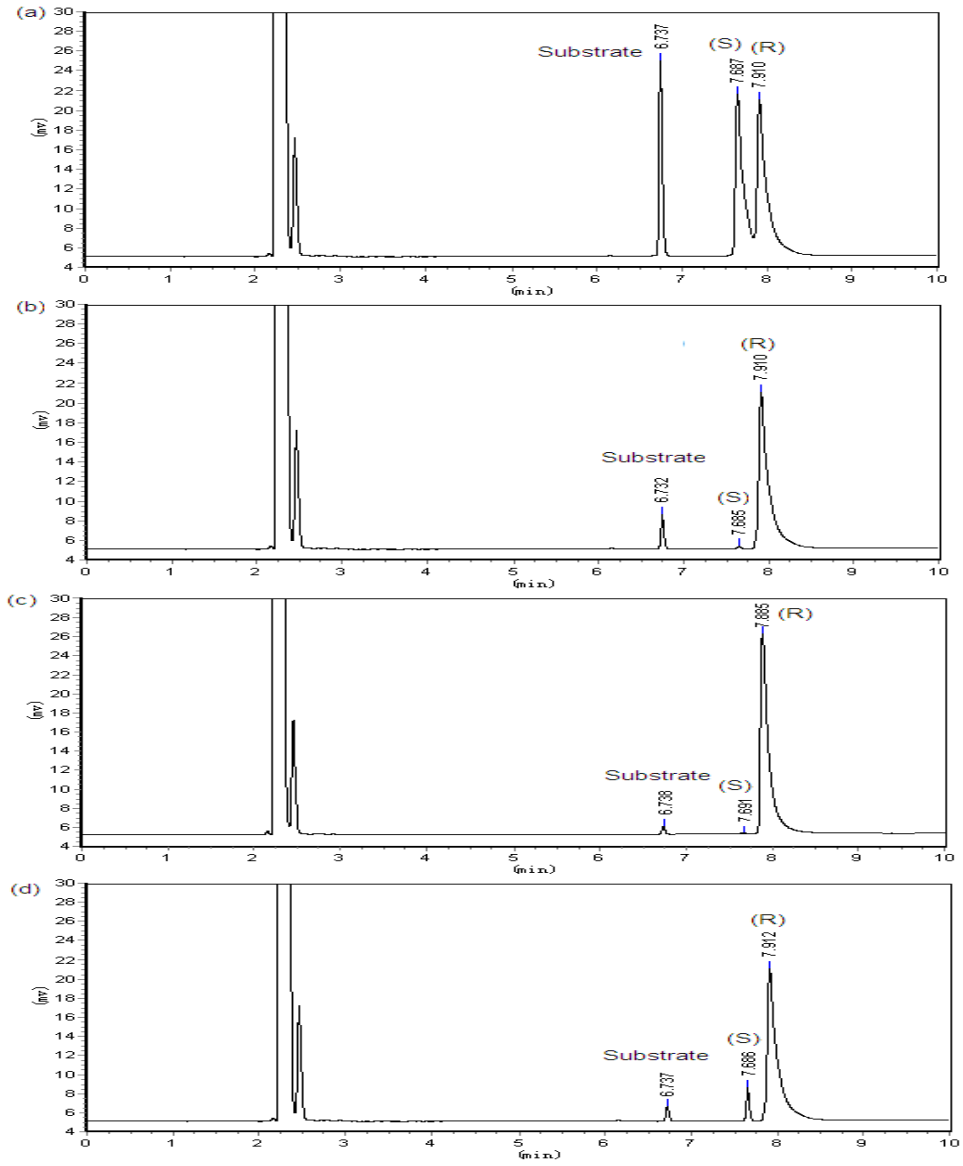

Figure S10. Chiral GC chromatograms of **10** and its corresponding chiral alcohols (a), the bioproducts catalyzed by *Bg*ADH1 (b), *Bg*ADH2 (c) and *Bg*ADH5 (d).

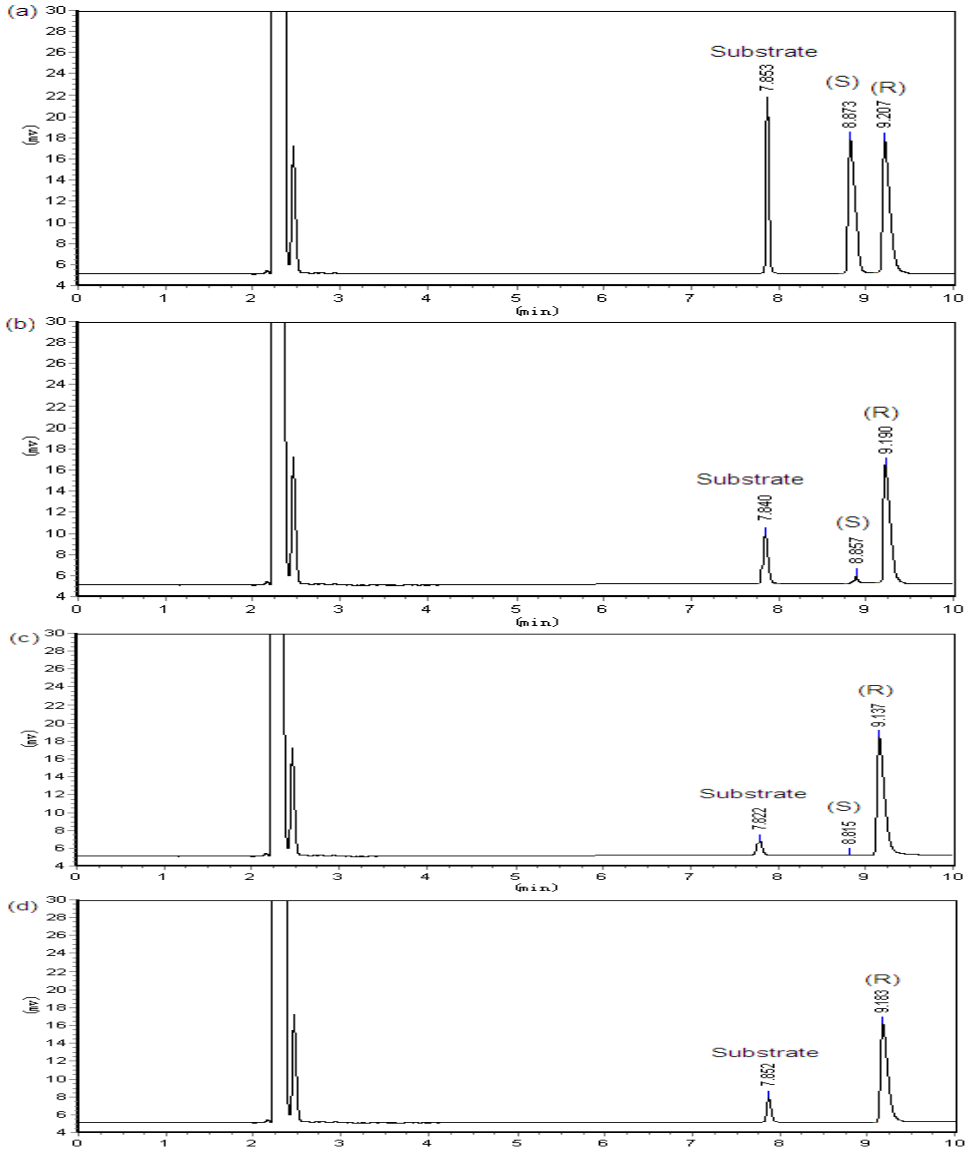

Figure S11. Chiral GC chromatograms of **11** and its corresponding chiral alcohols (a), the bioproducts catalyzed by *Bg*ADH1 (b), *Bg*ADH2 (c), and *Bg*ADH5 (d).

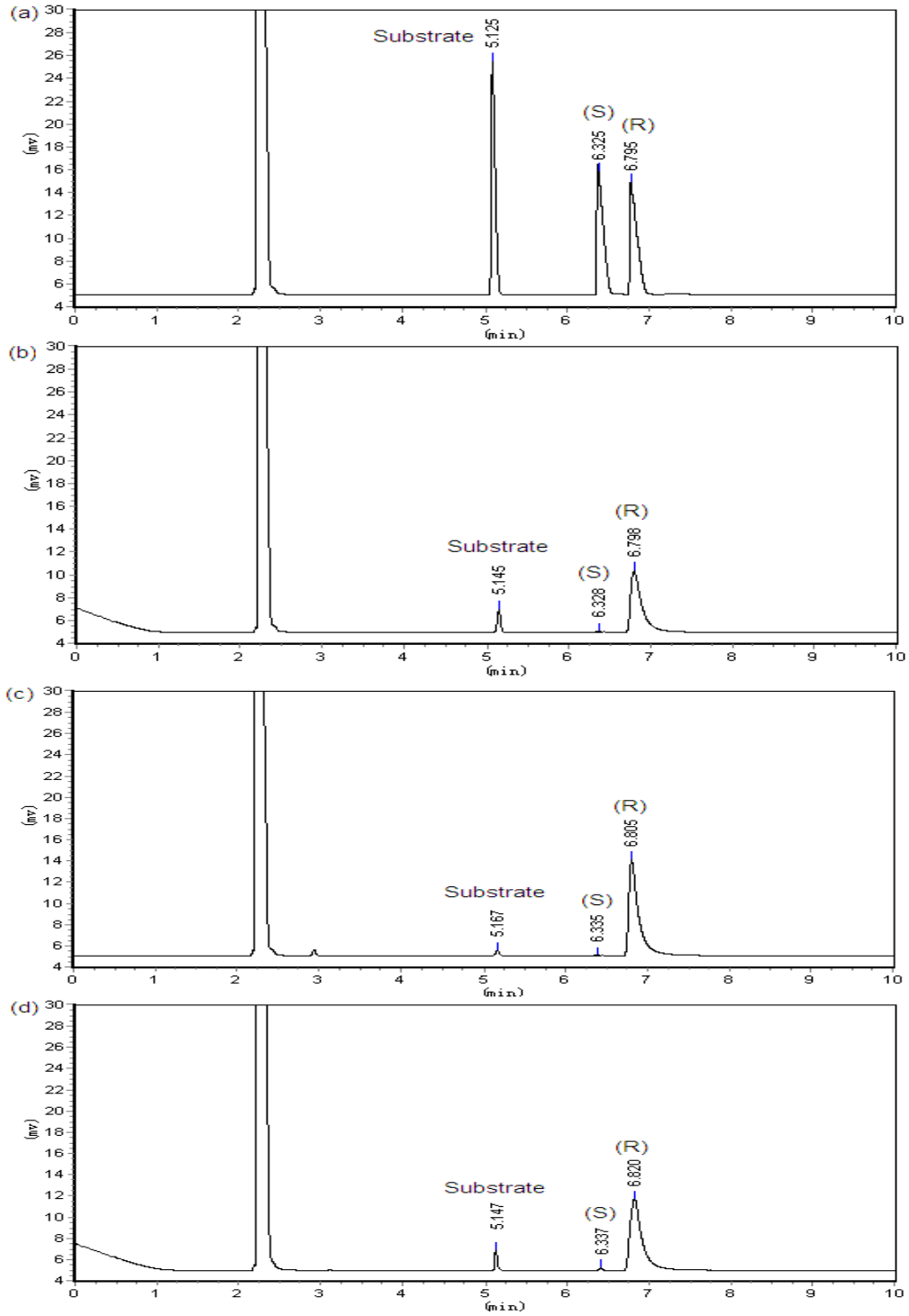

Figure S12. Chiral GC chromatograms of **15** and its corresponding chiral alcohols (a), the corresponding bioproducts catalyzed by *Bg*ADH1 (b), *Bg*ADH2 (c), and *Bg*ADH5 (d).

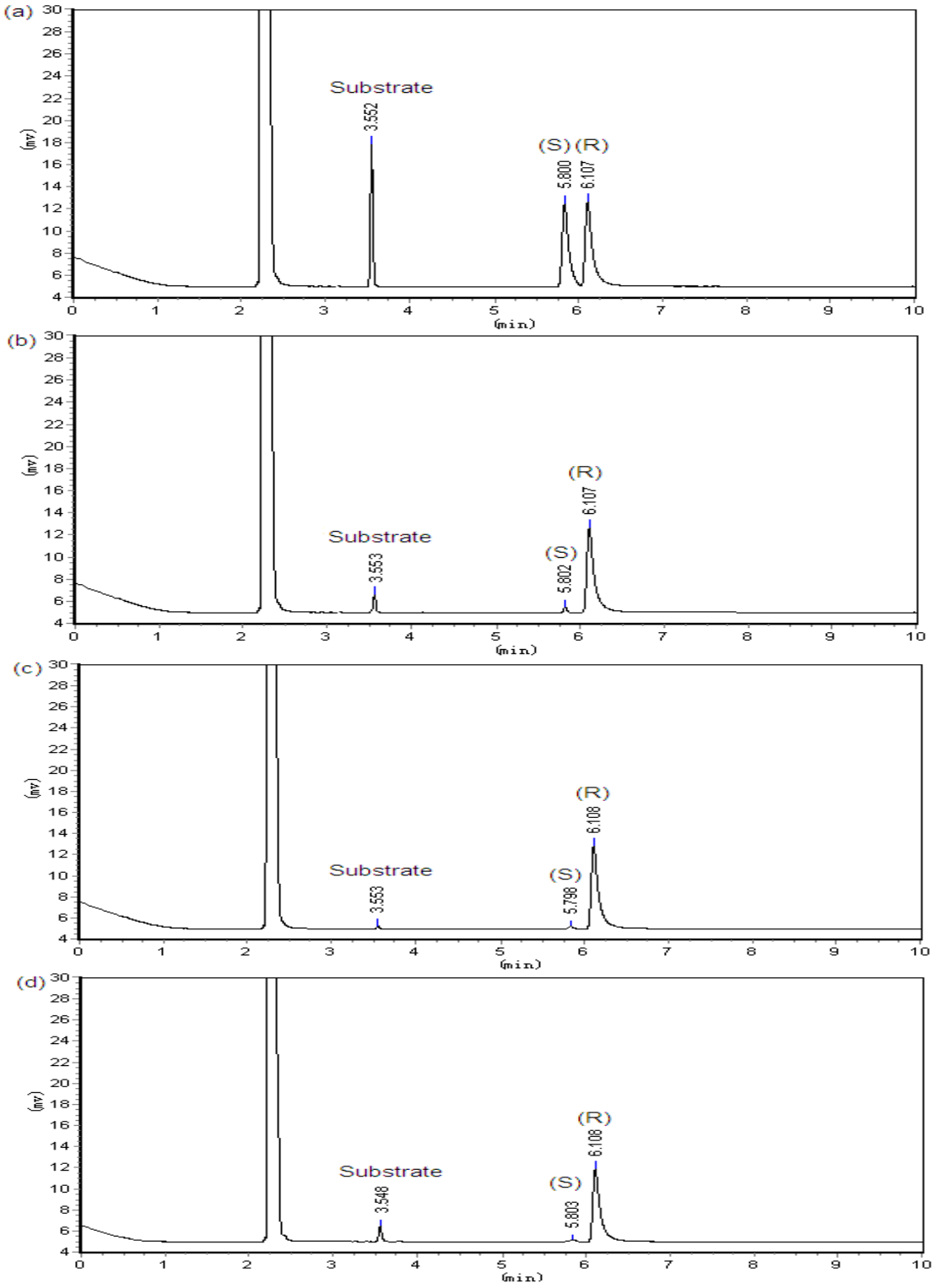

Figure S13. Chiral GC chromatograms of **16** and its corresponding chiral alcohols (a), the bioproducts catalyzed by *Bg*ADH1 (b), *Bg*ADH2 (c), and *Bg*ADH5 (d).

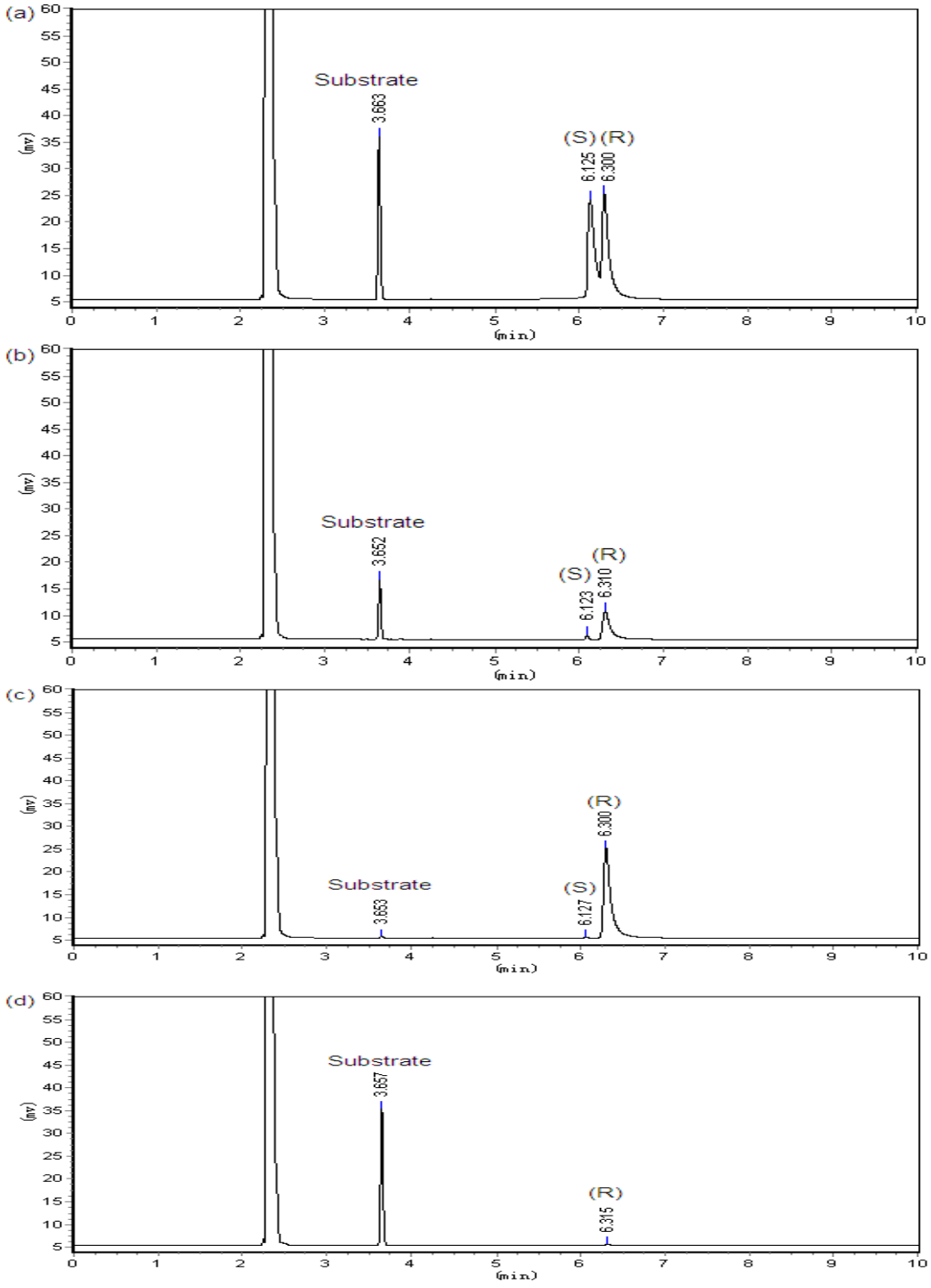

Figure S14. Chiral GC chromatograms of **17** and its corresponding chiral alcohols (a), the bioproducts catalyzed by *Bg*ADH1 (b), *Bg*ADH2 (c), and *Bg*ADH5 (d).

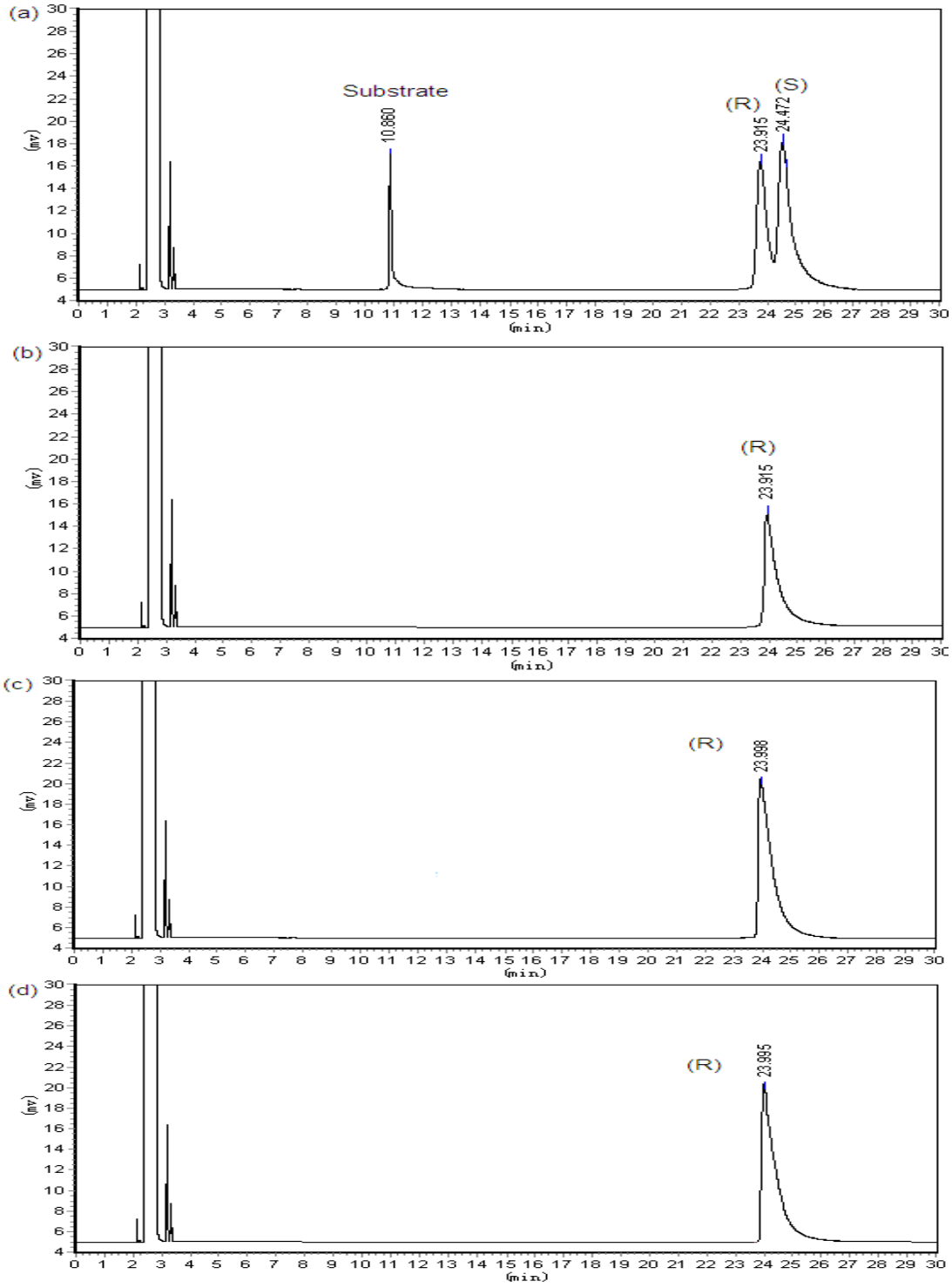

Figure S15. Chiral GC chromatograms of **23** and its corresponding chiral alcohols (a), the bioproducts catalyzed by *Bg*ADH1 (b), *Bg*ADH2 (c), and *Bg*ADH5 (d).

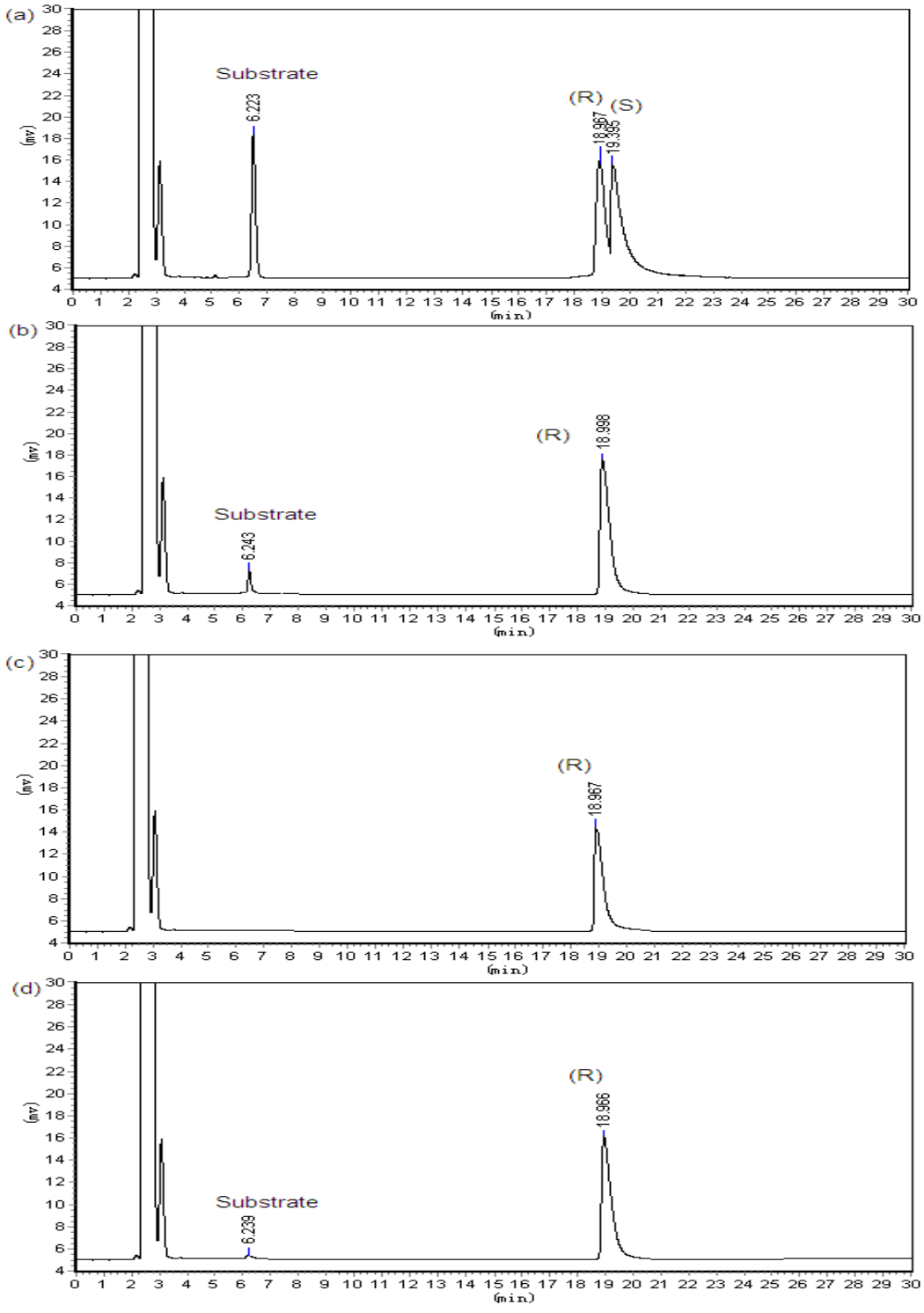

Figure S16. Chiral GC chromatograms of **24** and its corresponding chiral alcohols (a), the bioproducts catalyzed by *Bg*ADH1 (b), *Bg*ADH2 (c), and *Bg*ADH5 (d).

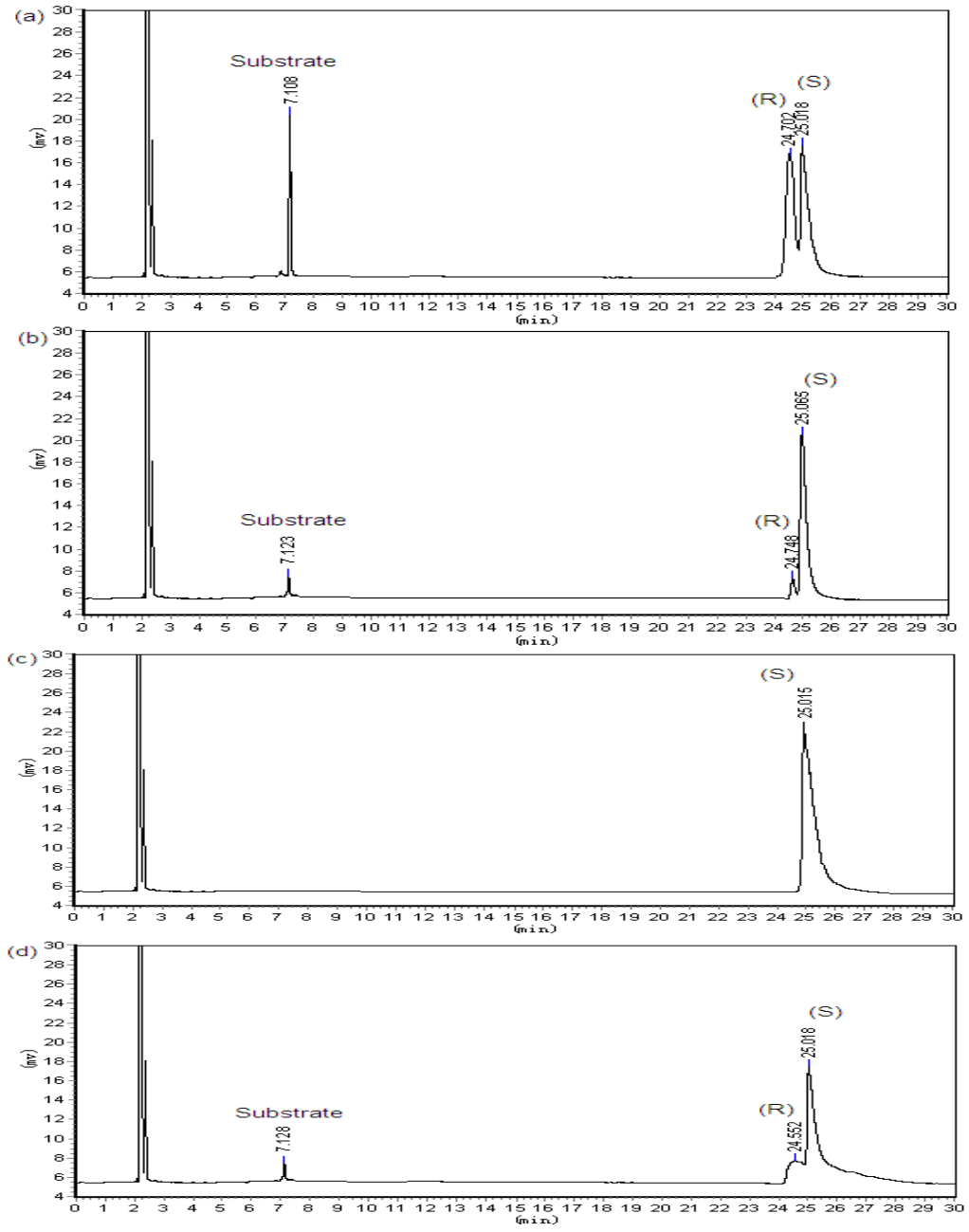

Figure S17. Chiral GC chromatograms of **25** and its corresponding chiral alcohols (a), the bioproducts catalyzed by *Bg*ADH1 (b), *Bg*ADH2 (c), and *Bg*ADH5 (d).

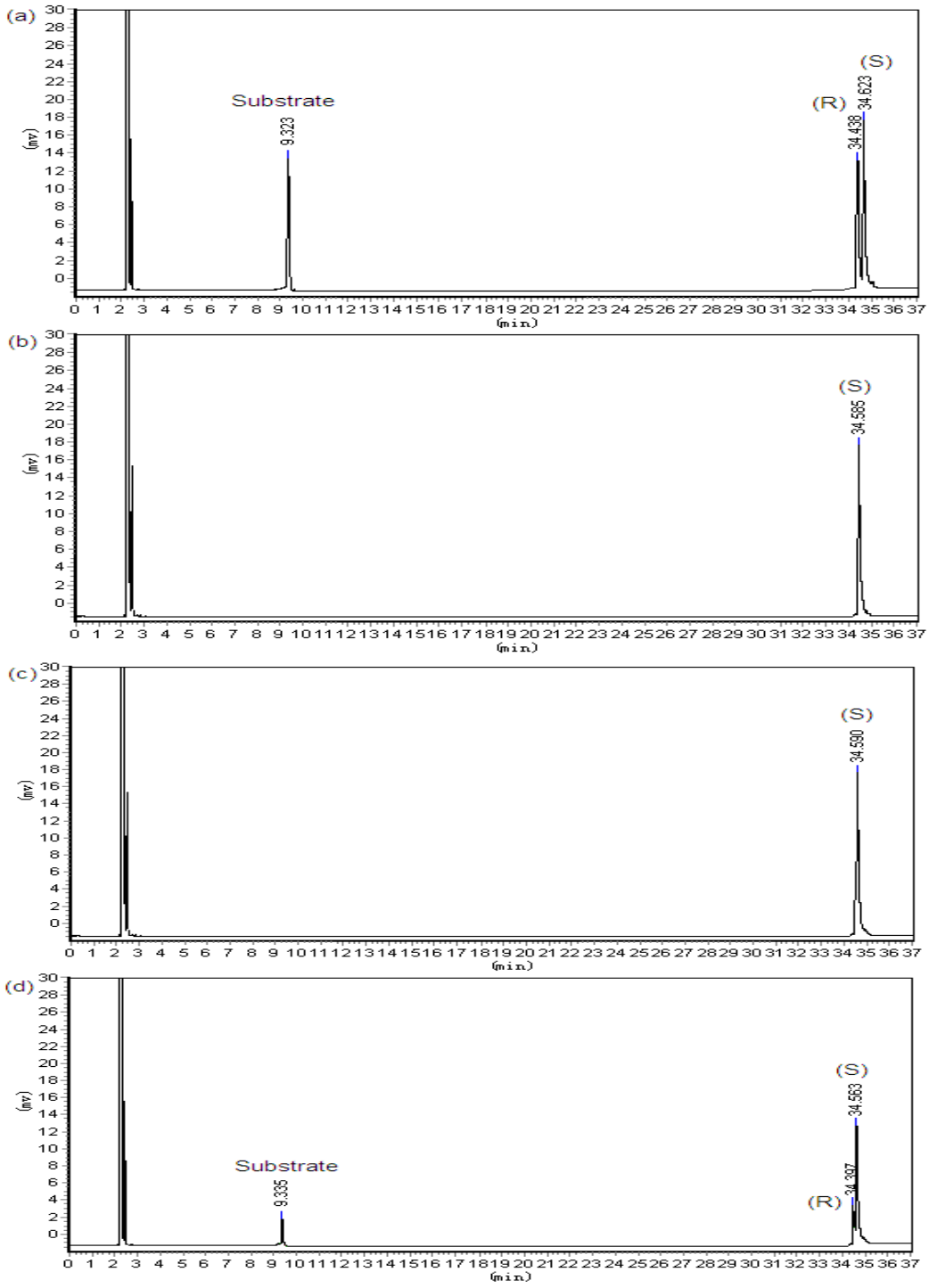

Figure S18. Chiral GC chromatograms of **26** and its corresponding chiral alcohols (a), the bioproducts catalyzed by *Bg*ADH1 (b), *Bg*ADH2 (c), and *Bg*ADH5 (d).

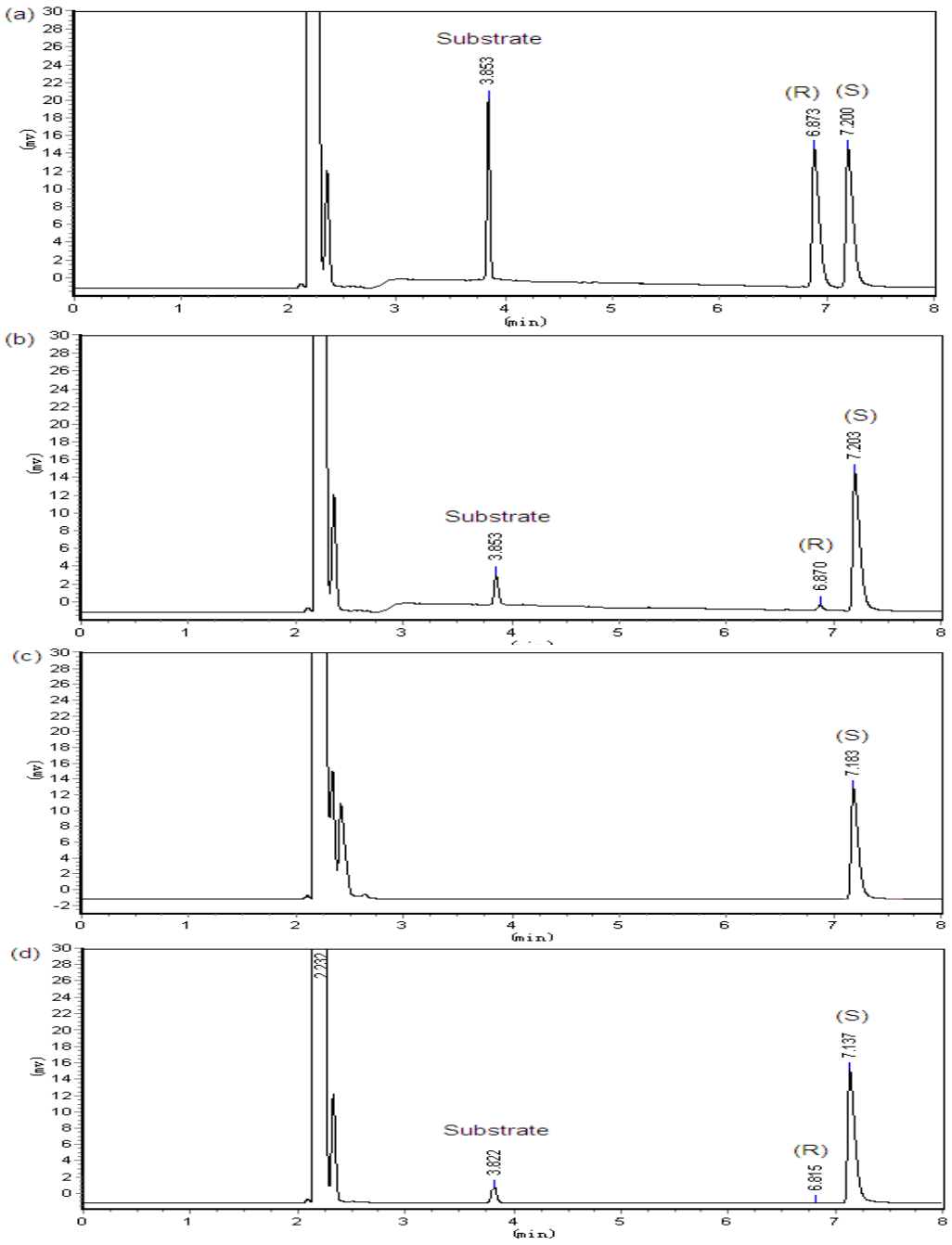

Figure S19. Chiral GC chromatograms of **27** and its corresponding chiral alcohols (a), the bioproducts catalyzed by *Bg*ADH1 (b), *Bg*ADH2 (c), and *Bg*ADH5 (d).

17. Chiral HPLC chromatograms

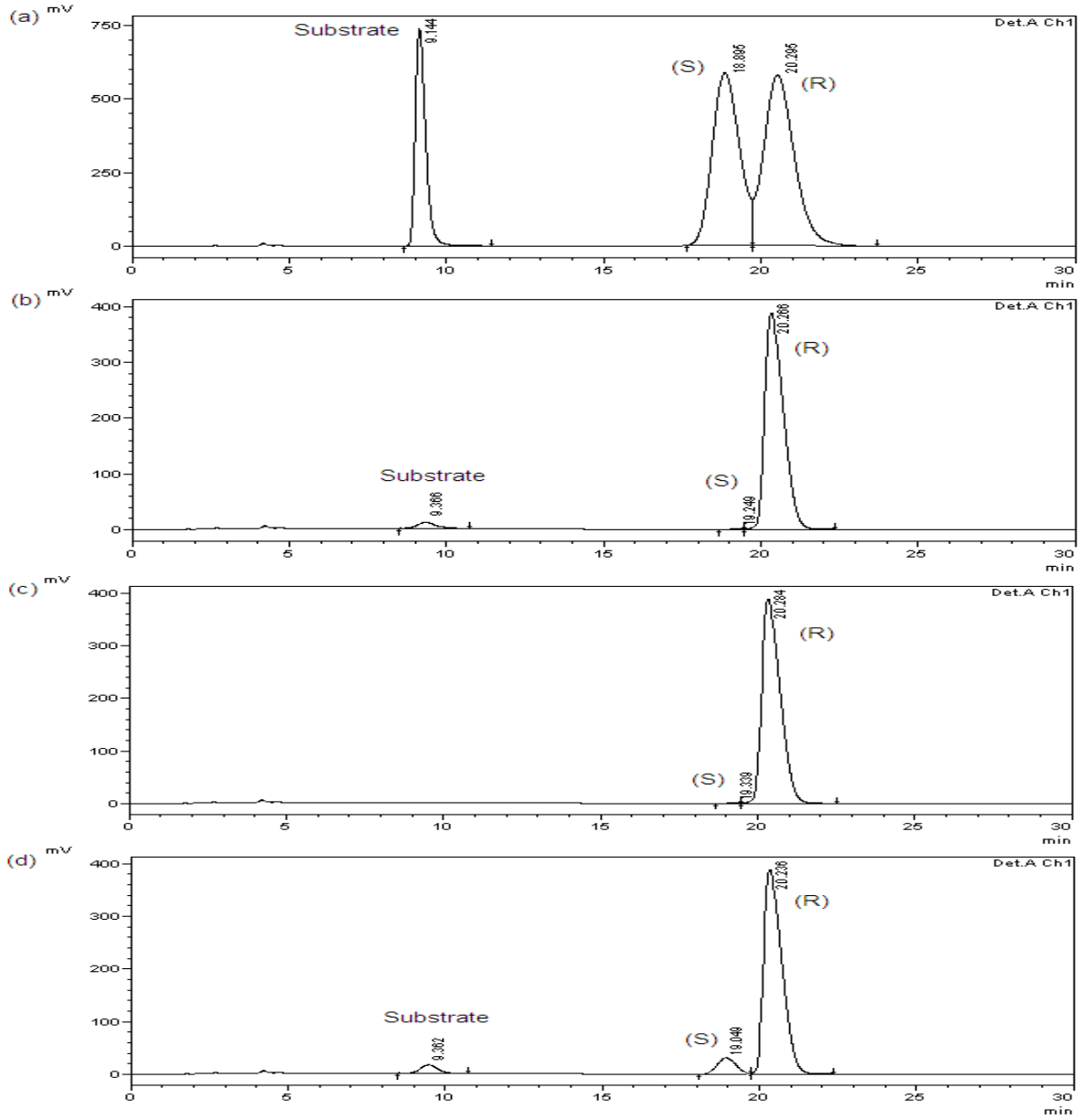

Figure S20. Chiral HPLC chromatograms of **12** and its corresponding chiral alcohols (a), the bioproducts catalyzed by *Bg*ADH1 (b), *Bg*ADH2 (c), and *Bg*ADH5 (d).

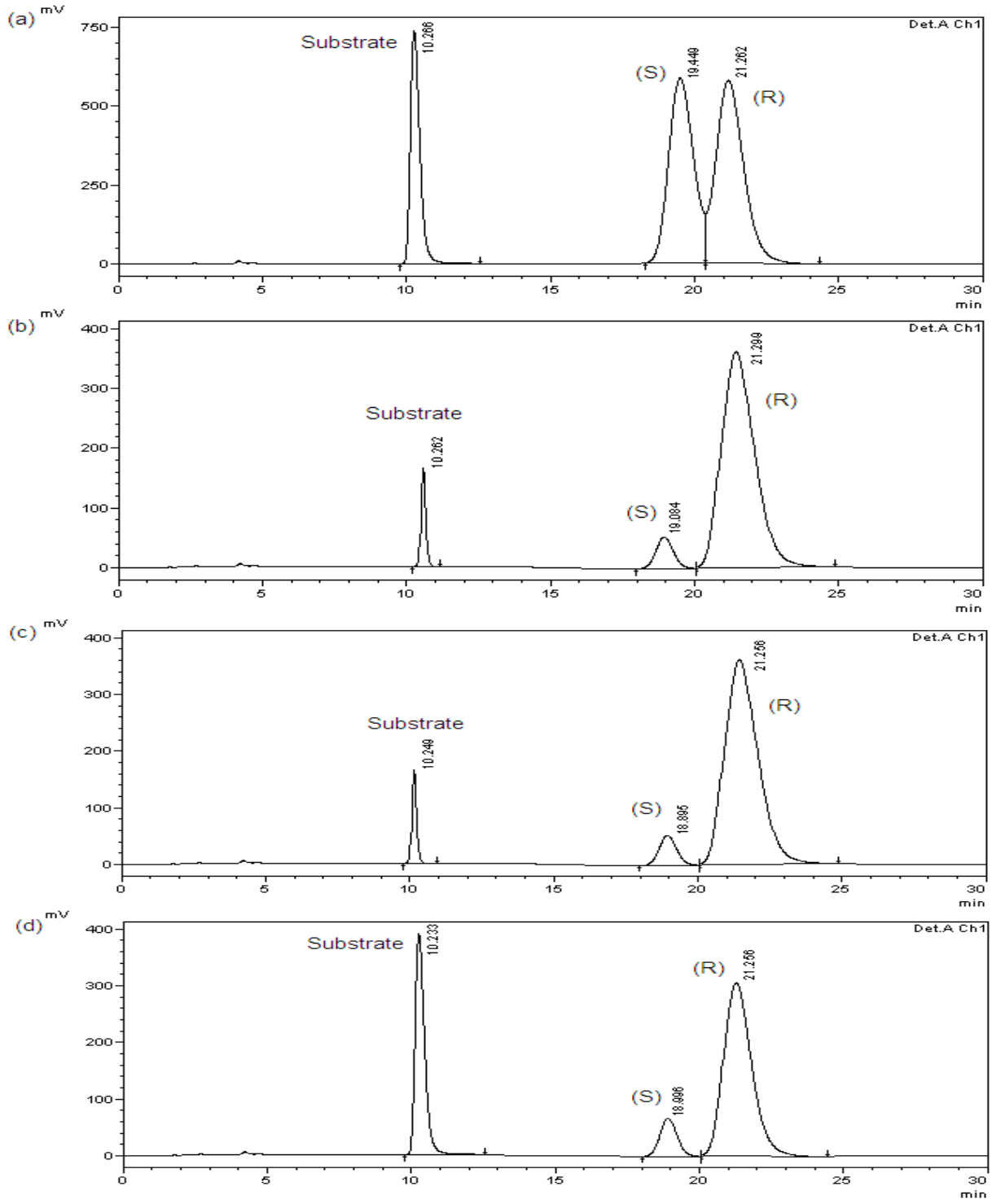

Figure S21. Chiral HPLC chromatograms of **13** and its corresponding chiral alcohols (a), the bioproducts catalyzed by *Bg*ADH1 (b), *Bg*ADH2 (c), and *Bg*ADH5 (d).

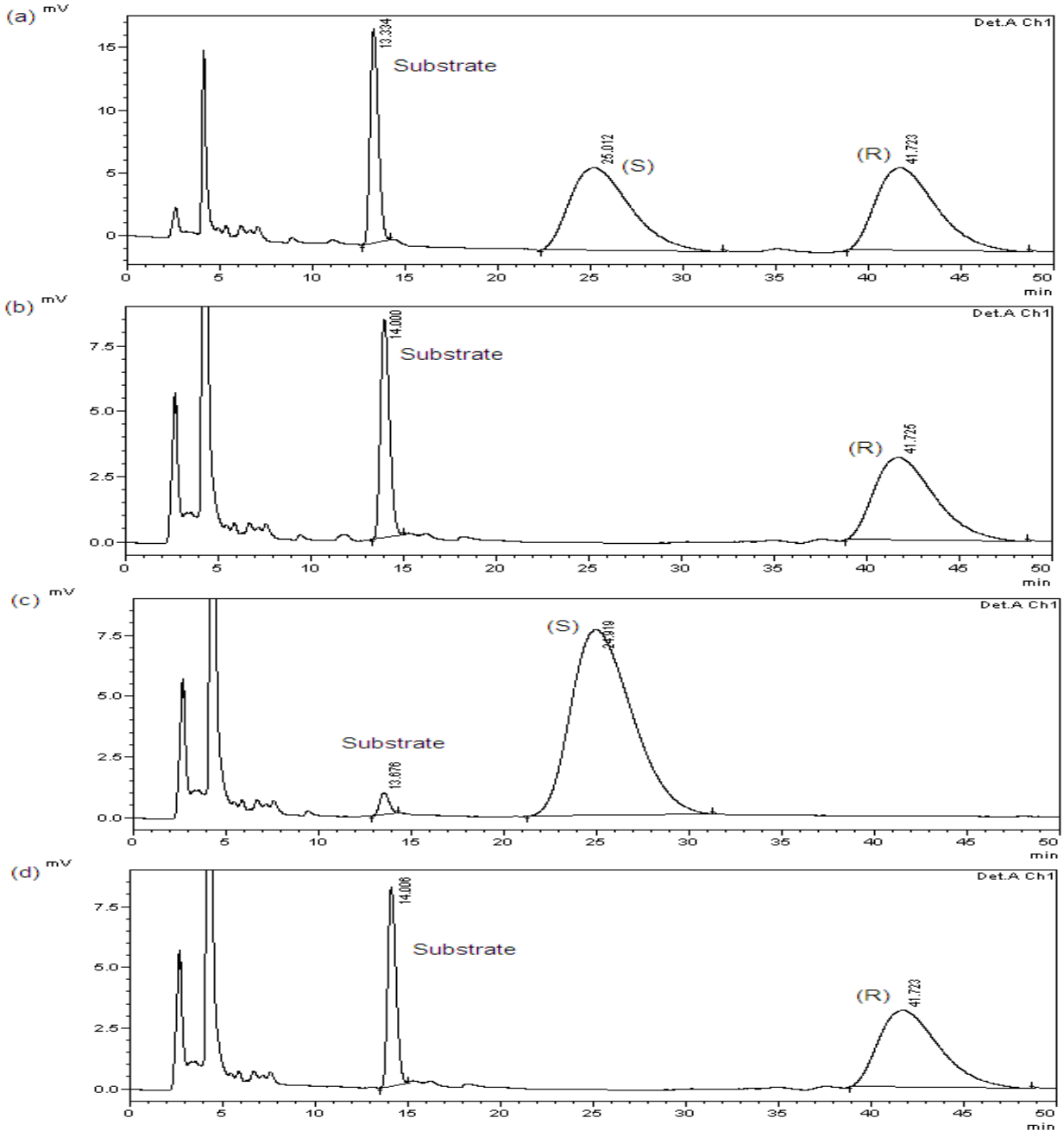

Figure S22. Chiral HPLC chromatograms of **14** and its corresponding chiral alcohols (a), the bioproducts catalyzed by *Bg*ADH1 (b), *Bg*ADH2 (c), and *Bg*ADH5 (d).

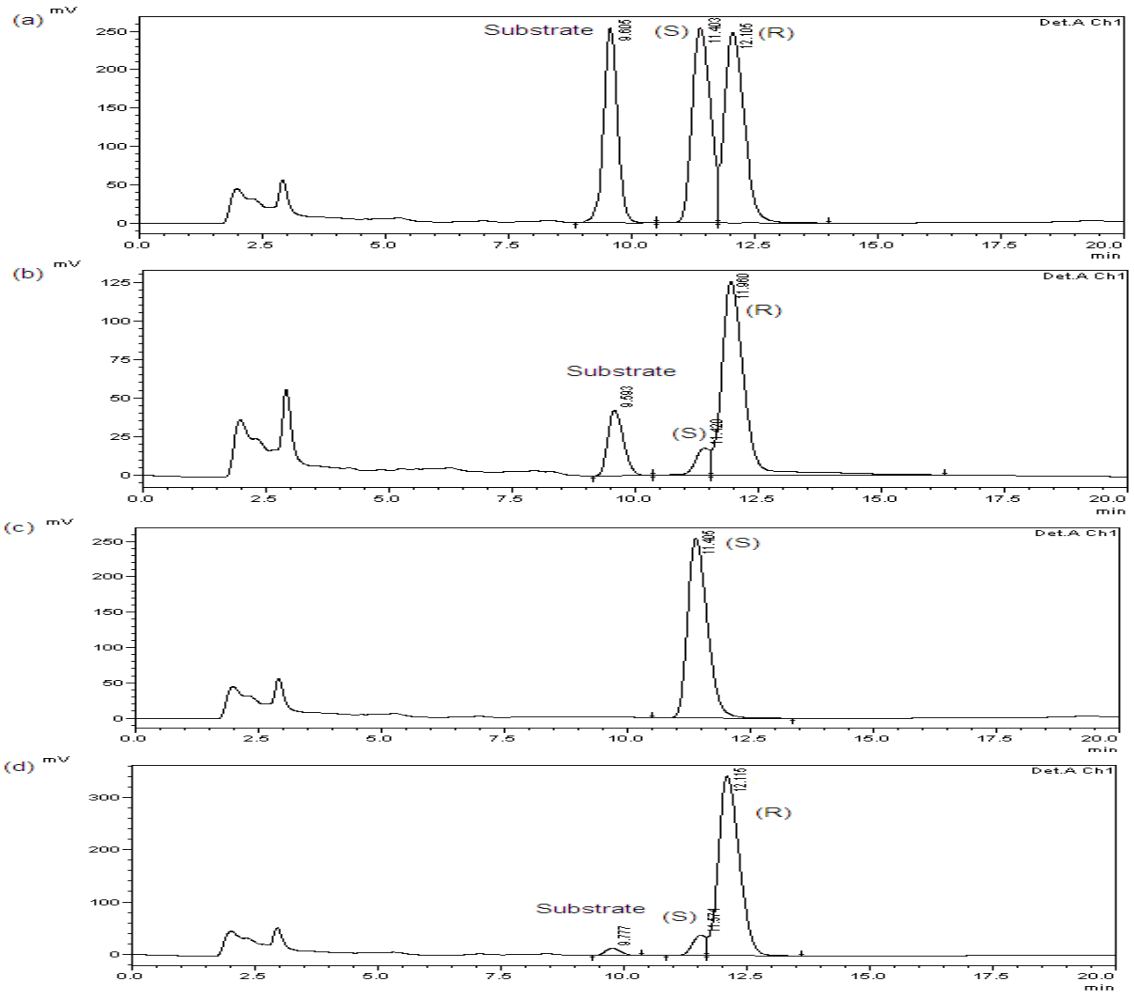

Figure S23. Chiral HPLC chromatograms of **18** and its corresponding chiral alcohols (a), the bioproducts catalyzed by *Bg*ADH1 (b), *Bg*ADH2 (c), and *Bg*ADH5 (d).

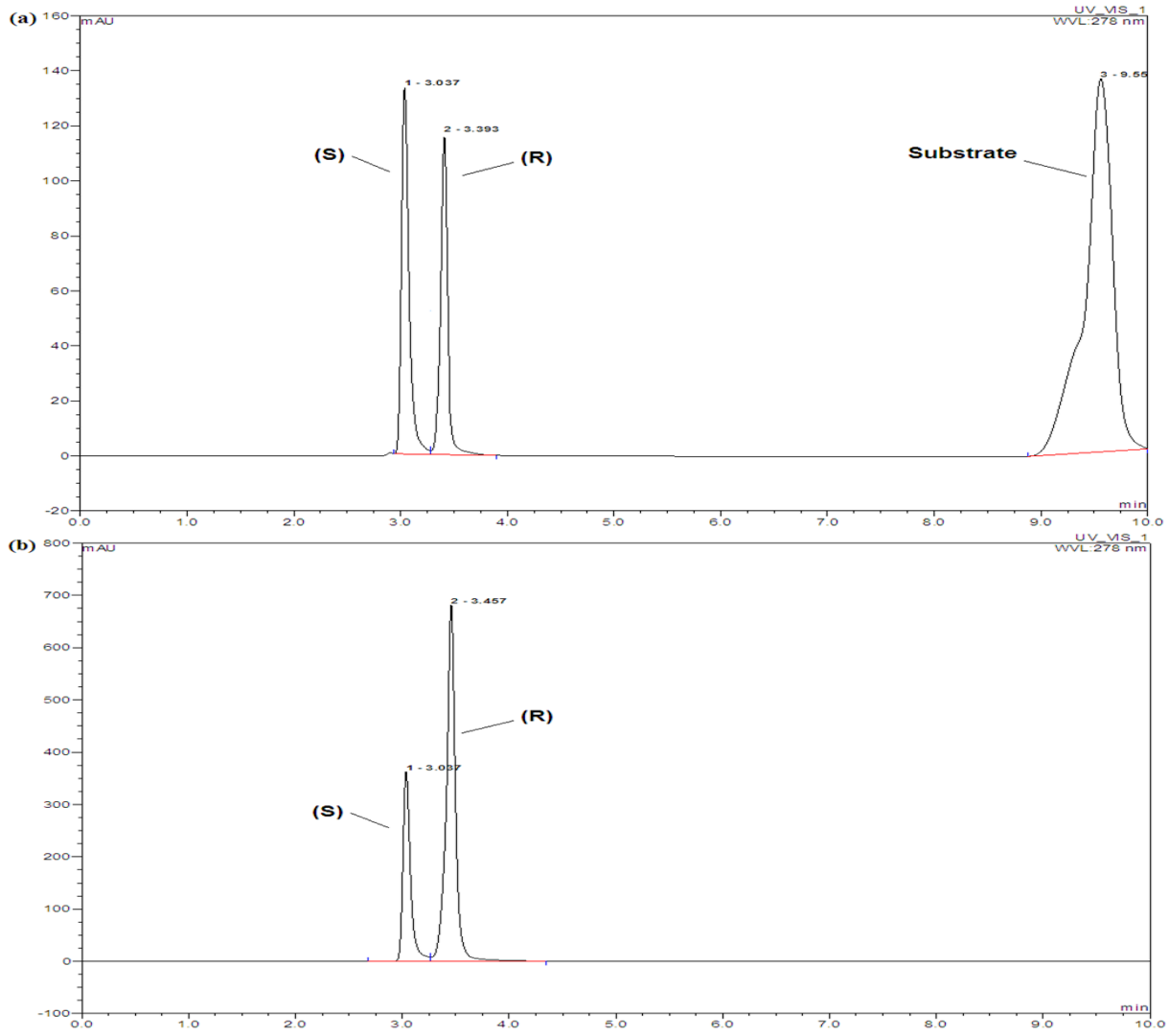

Figure S24. Chiral HPLC chromatograms of **20** and its corresponding chiral alcohols (a), the bioproducts catalyzed by *Bg*ADH2 (b).

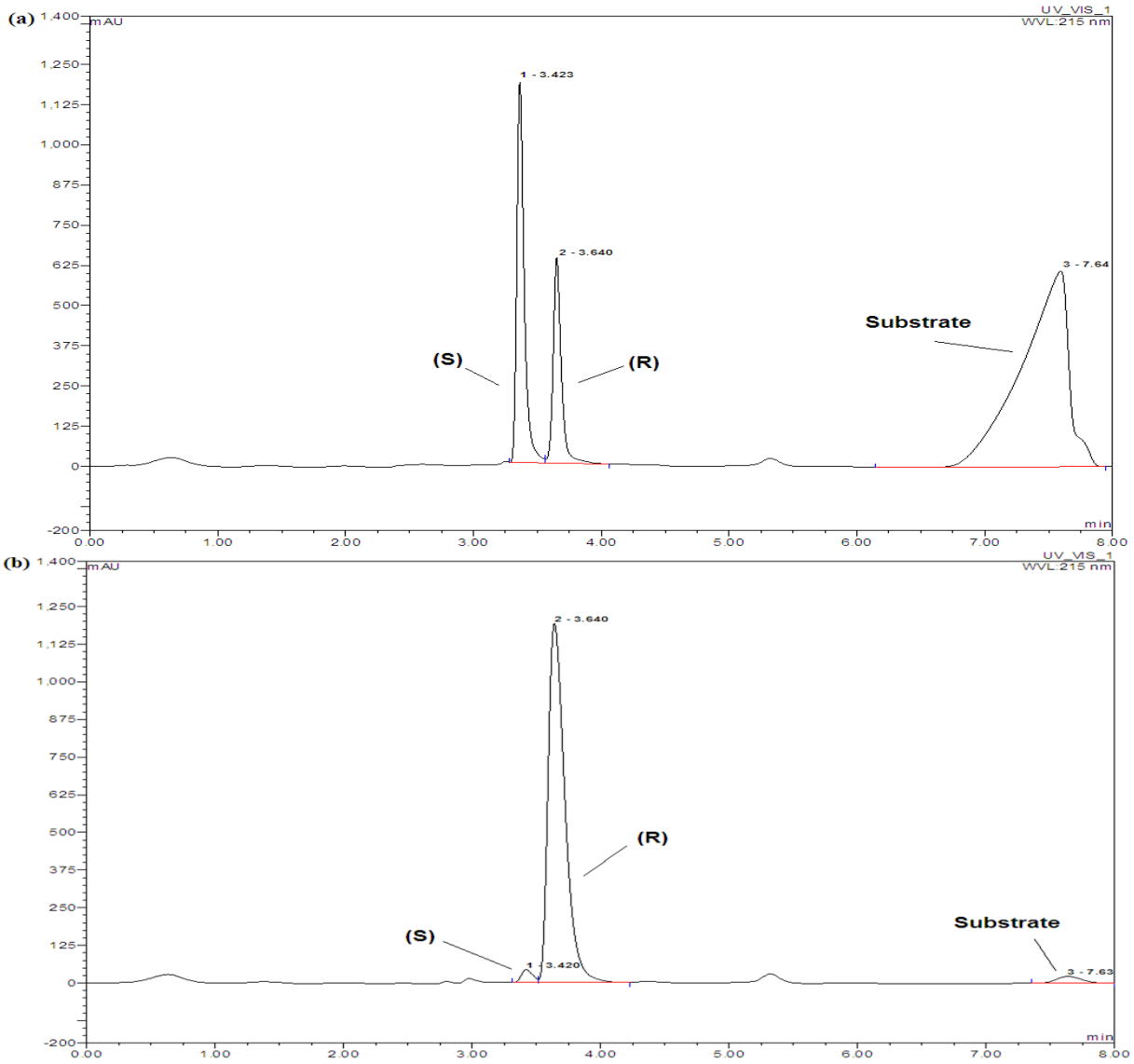

Figure S25. Chiral HPLC chromatograms of **21** and its corresponding chiral alcohols (a), the bioproducts catalyzed by *Bg*ADH2 (b).

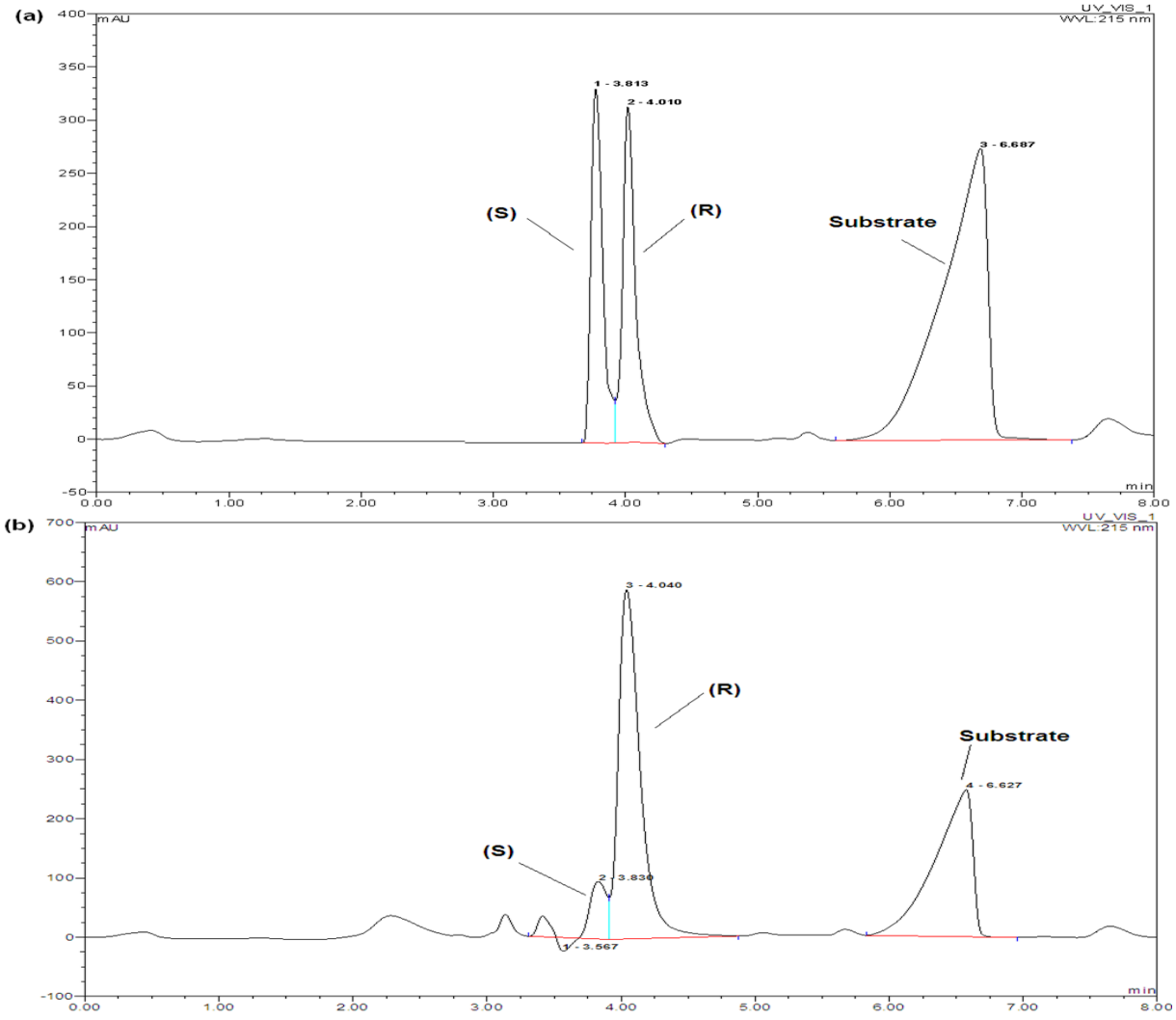

Figure S26. Chiral HPLC chromatograms of **22** and its corresponding chiral alcohols (a), the bioproducts catalyzed by *Bg*ADH2 (b).

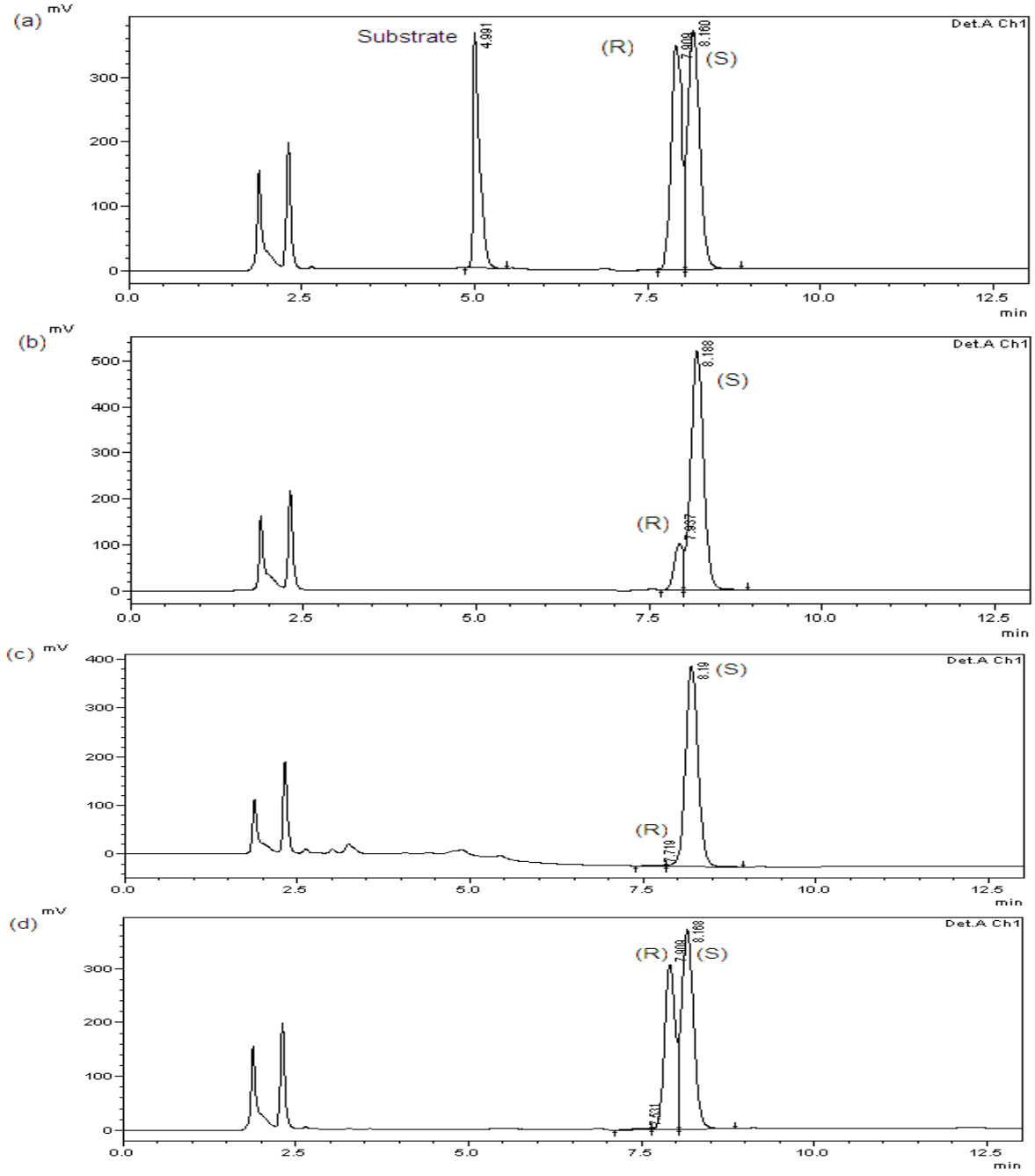

Figure S27. Chiral HPLC chromatograms of **28** and its corresponding chiral alcohols (a), the bioproducts catalyzed by *Bg*ADH1 (b), *Bg*ADH2 (c), and *Bg*ADH5 (d).

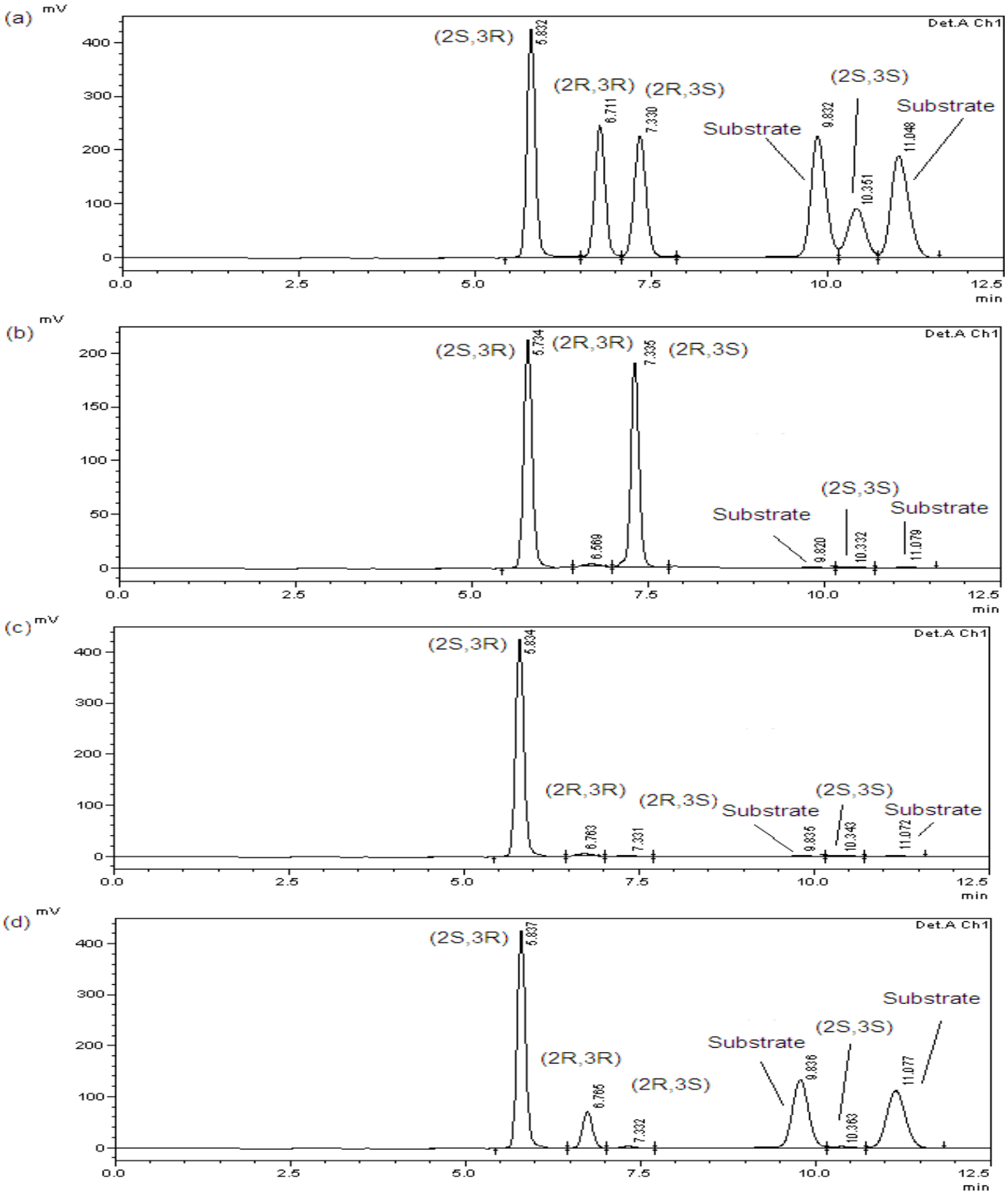

Figure S28. Chiral HPLC chromatograms of **29** (a) and its corresponding chiral alcohols (a), the bioproducts catalyzed by *Bg*ADH1 (b), *Bg*ADH2 (c), and *Bg*ADH5 (d).

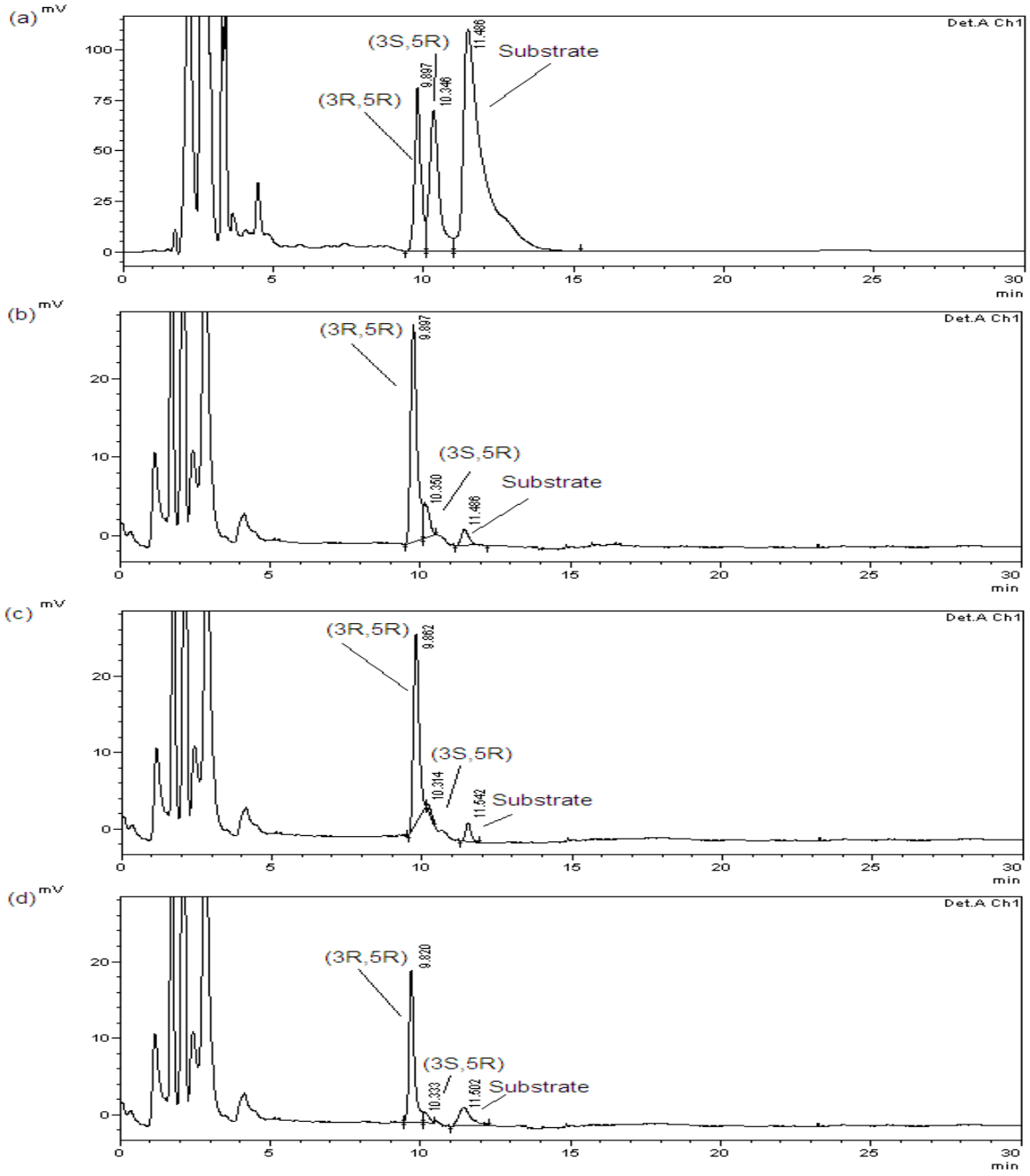

Figure S29. Chiral HPLC chromatograms of **30** and its corresponding chiral alcohols (a), the bioproducts catalyzed by *Bg*ADH1 (b), *Bg*ADH2 (c), and *Bg*ADH5 (d).

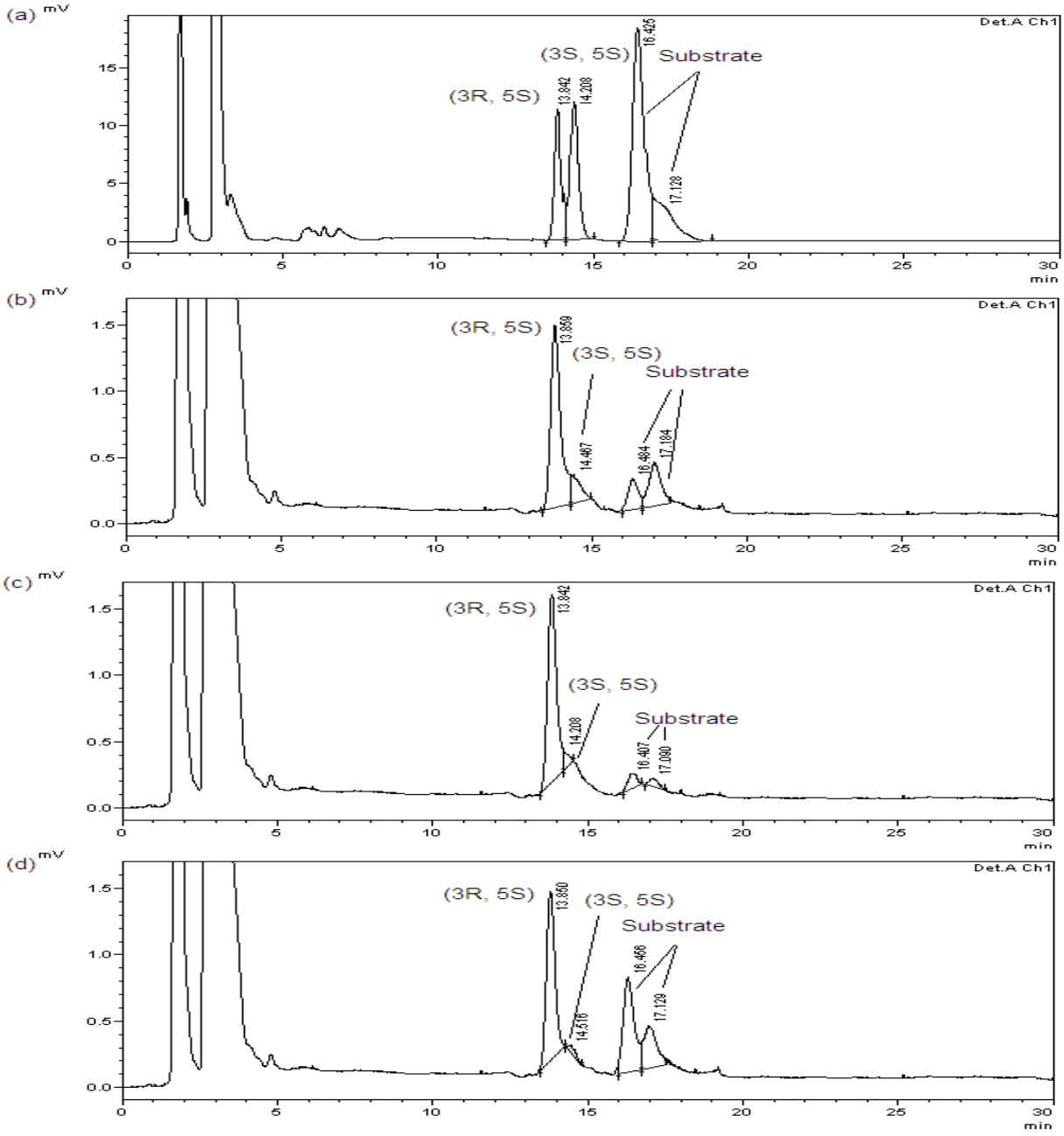

Figure S30. Chiral HPLC chromatograms of **31** and its corresponding chiral alcohols (a), the bioproducts catalyzed by *Bg*ADH1 (b), *Bg*ADH2 (c), and *Bg*ADH5 (d).

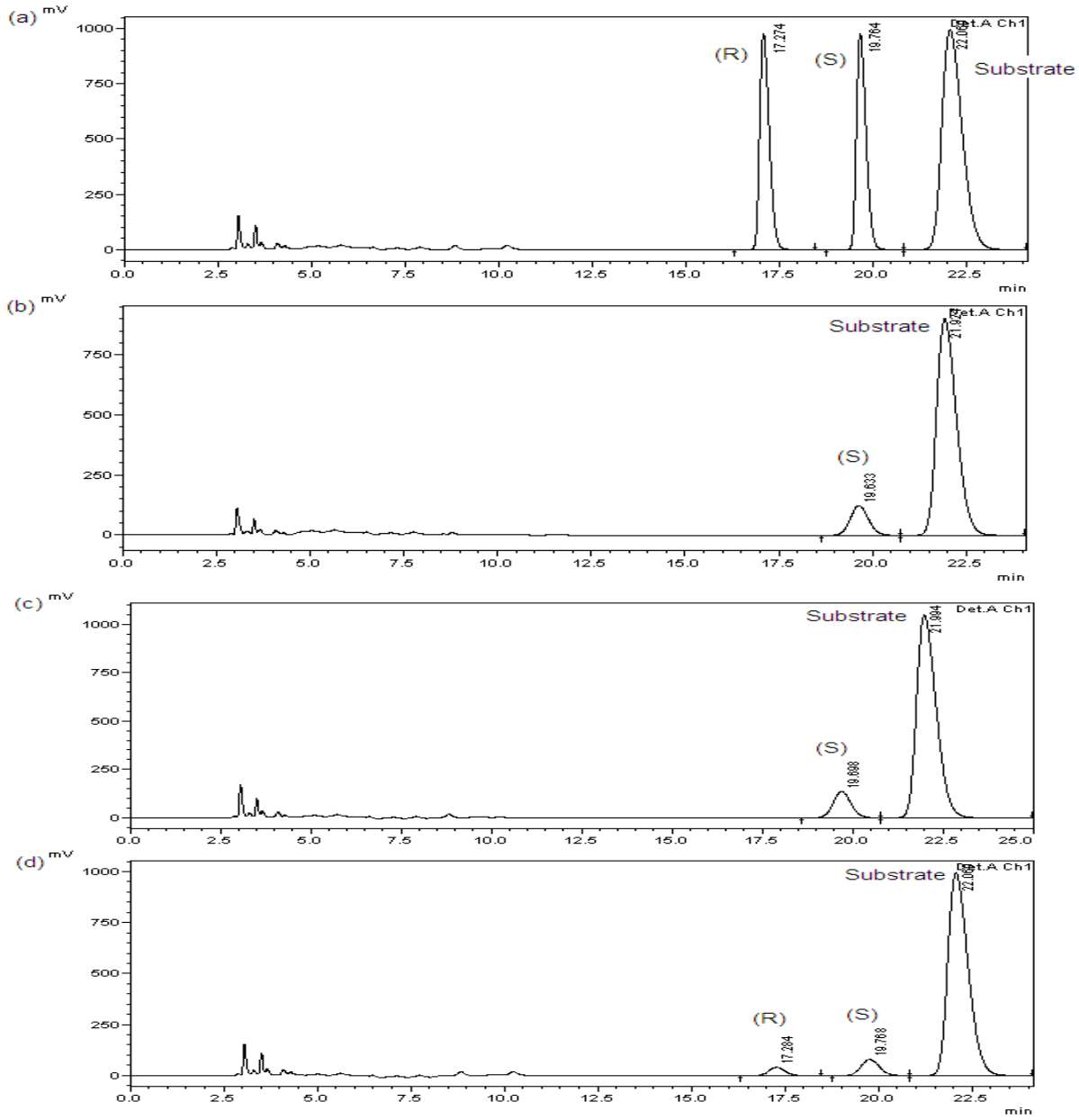

Figure S31. Chiral HPLC chromatograms of **32** and its corresponding chiral alcohols (a), the bioproducts catalyzed by *Bg*ADH1 (b), *Bg*ADH2 (c), and *Bg*ADH5 (d).

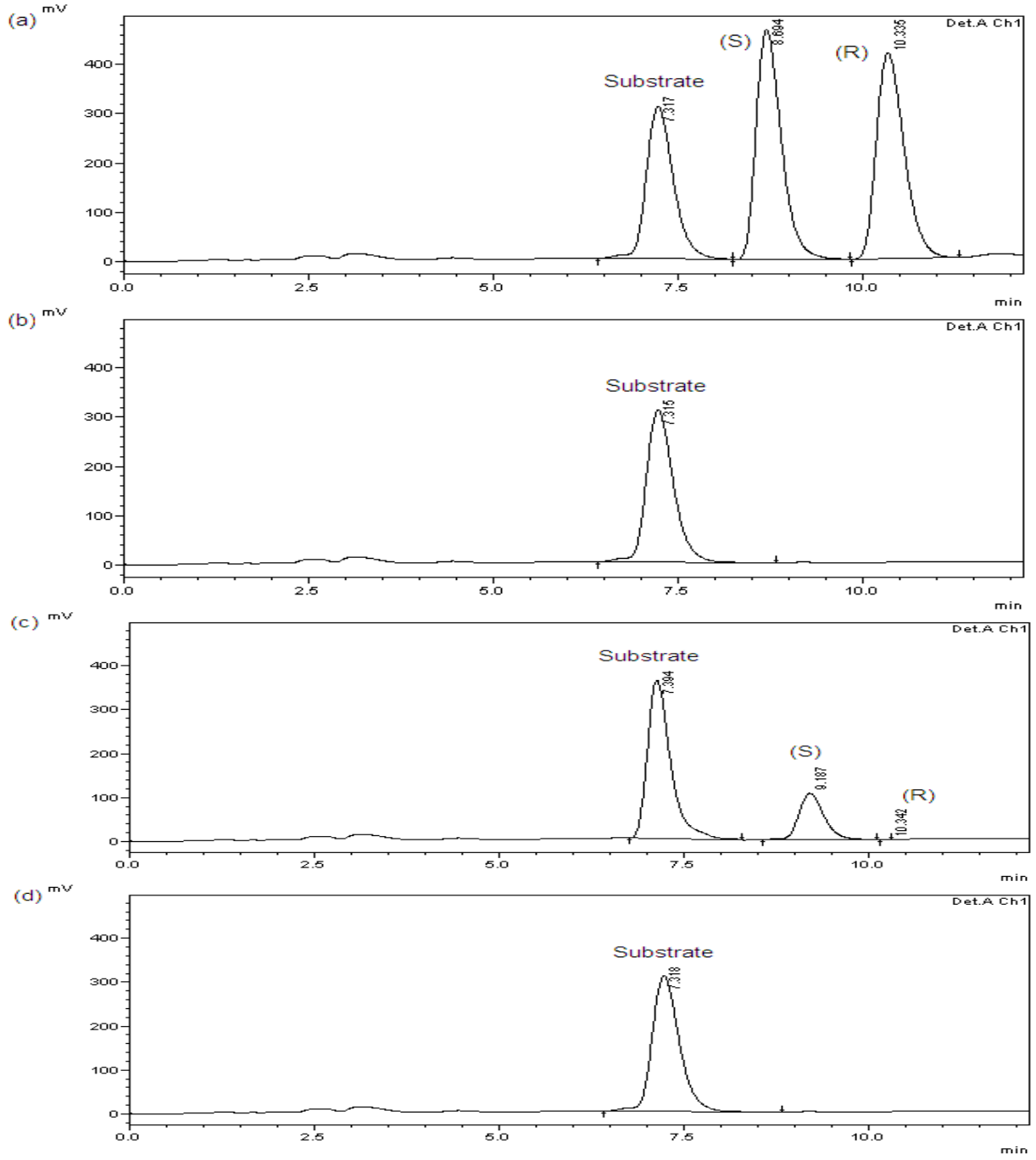

Figure S32. Chiral HPLC chromatograms of **34** (a) and its corresponding chiral alcohols (a), the bioproducts catalyzed by *Bg*ADH1 (b), *Bg*ADH2 (c), and *Bg*ADH5 (d).

18. NMR spectra of BMOB and MBHB

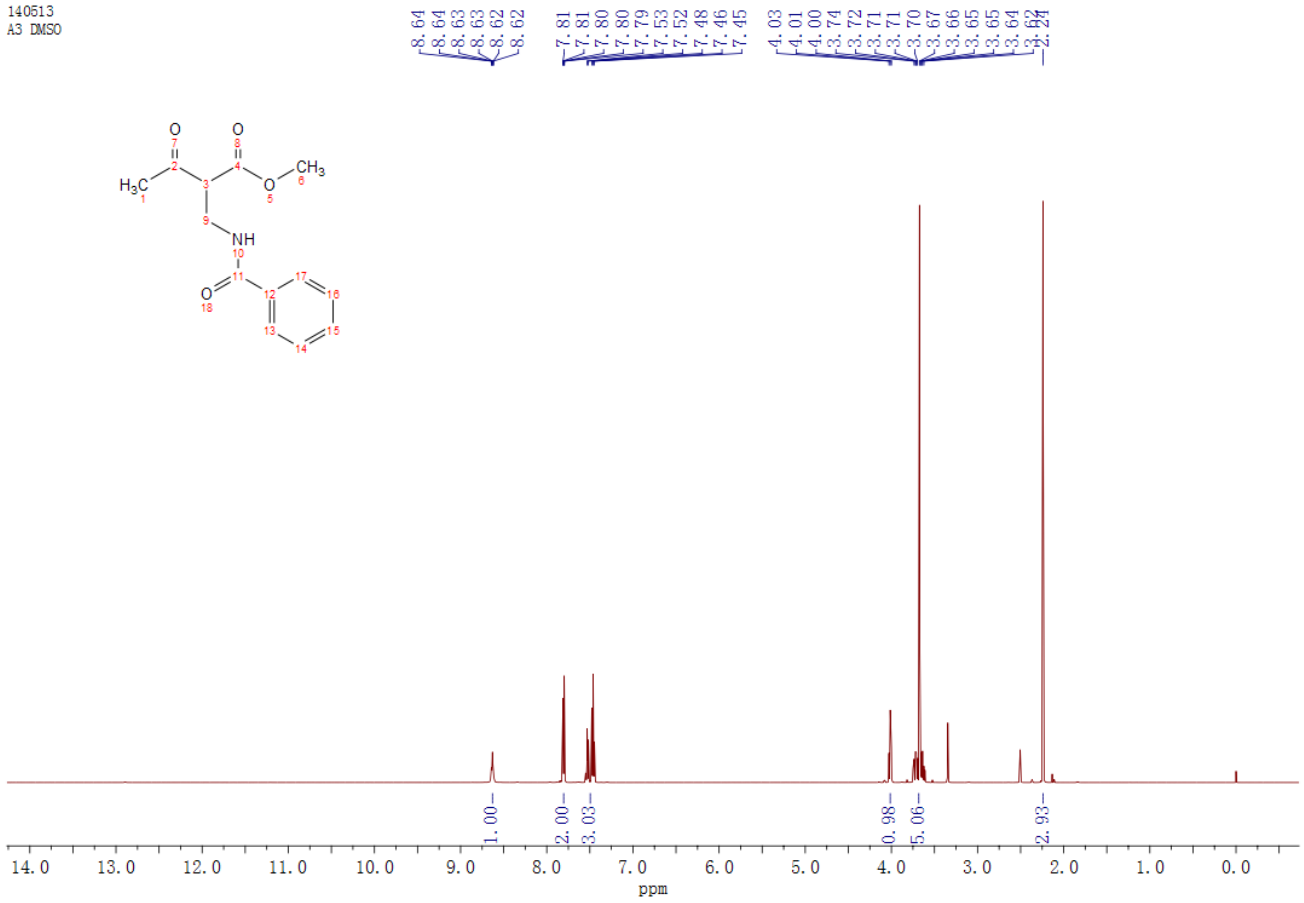

Figure S33. ^{1}H NMR spectrum of BMOB synthesized according to a modified literature procedure (500 MHz, DMSO-d_6).

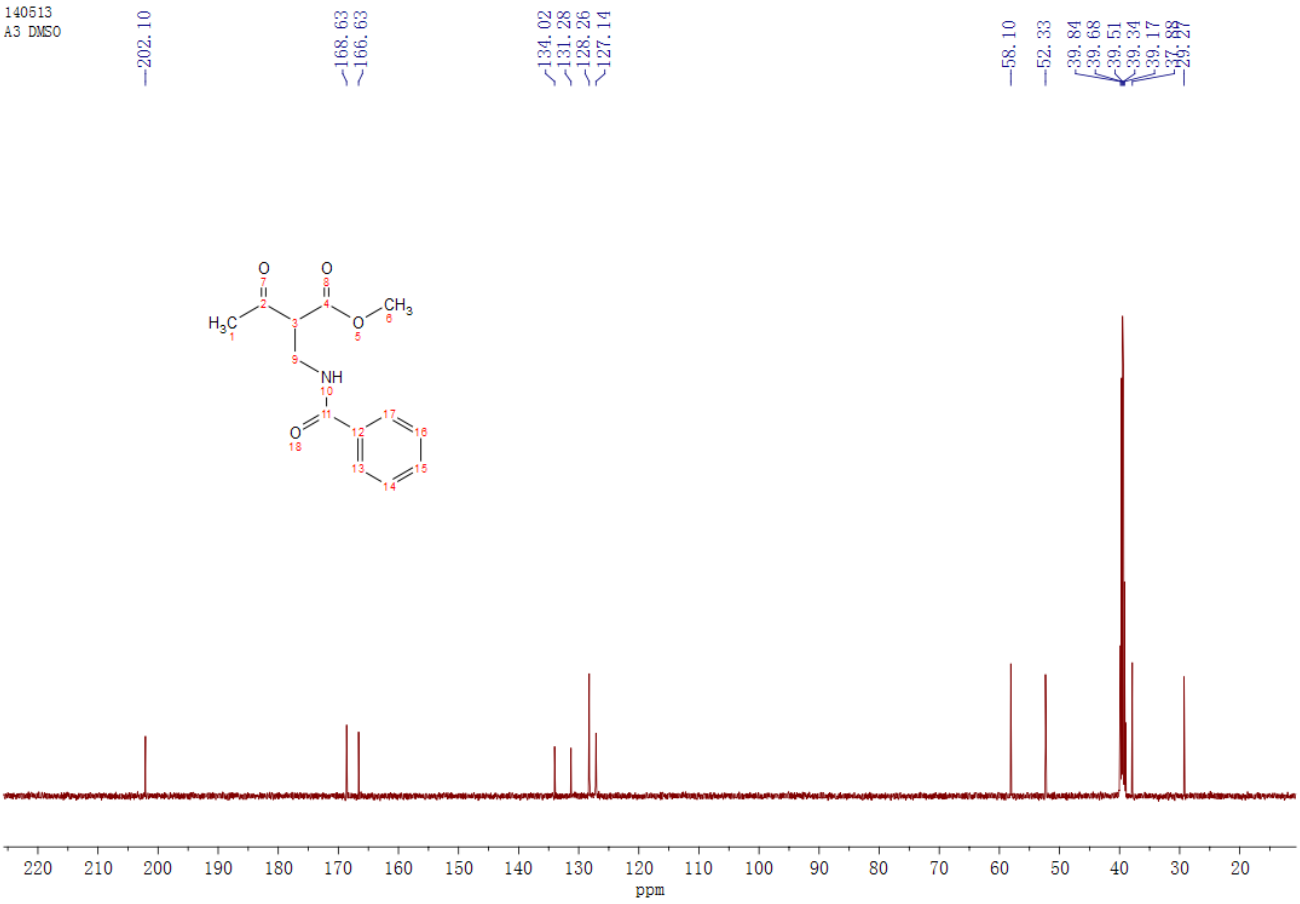

Figure S34. ^{13}C NMR spectrum of BMOB synthesized according to a modified literature procedure (126 MHz, DMSO-d_6).

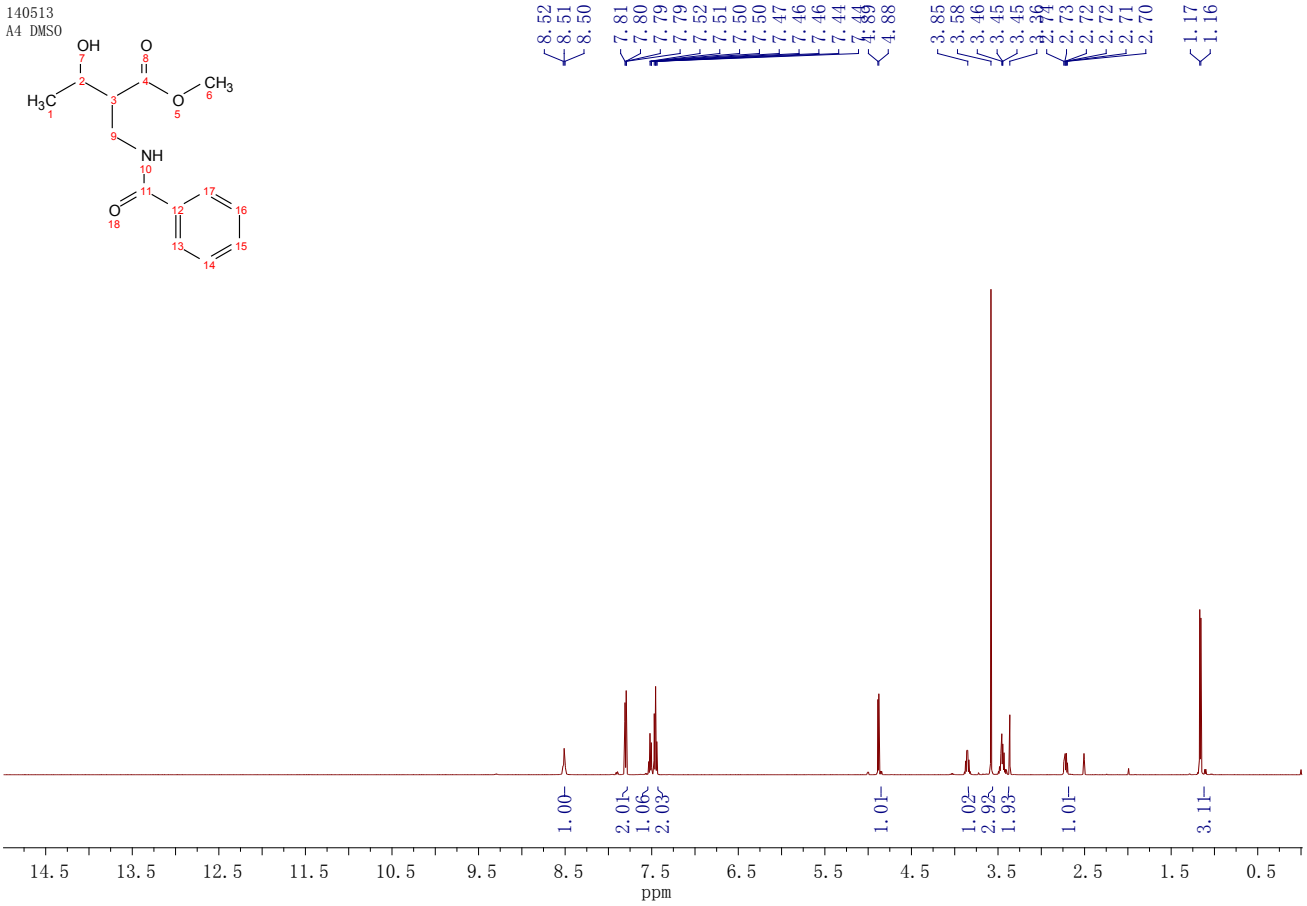

Figure S35. ^{1}H NMR spectrum of MBHB synthesized by $NaBH_4$ reduction (500 MHz, DMSO-d_6).

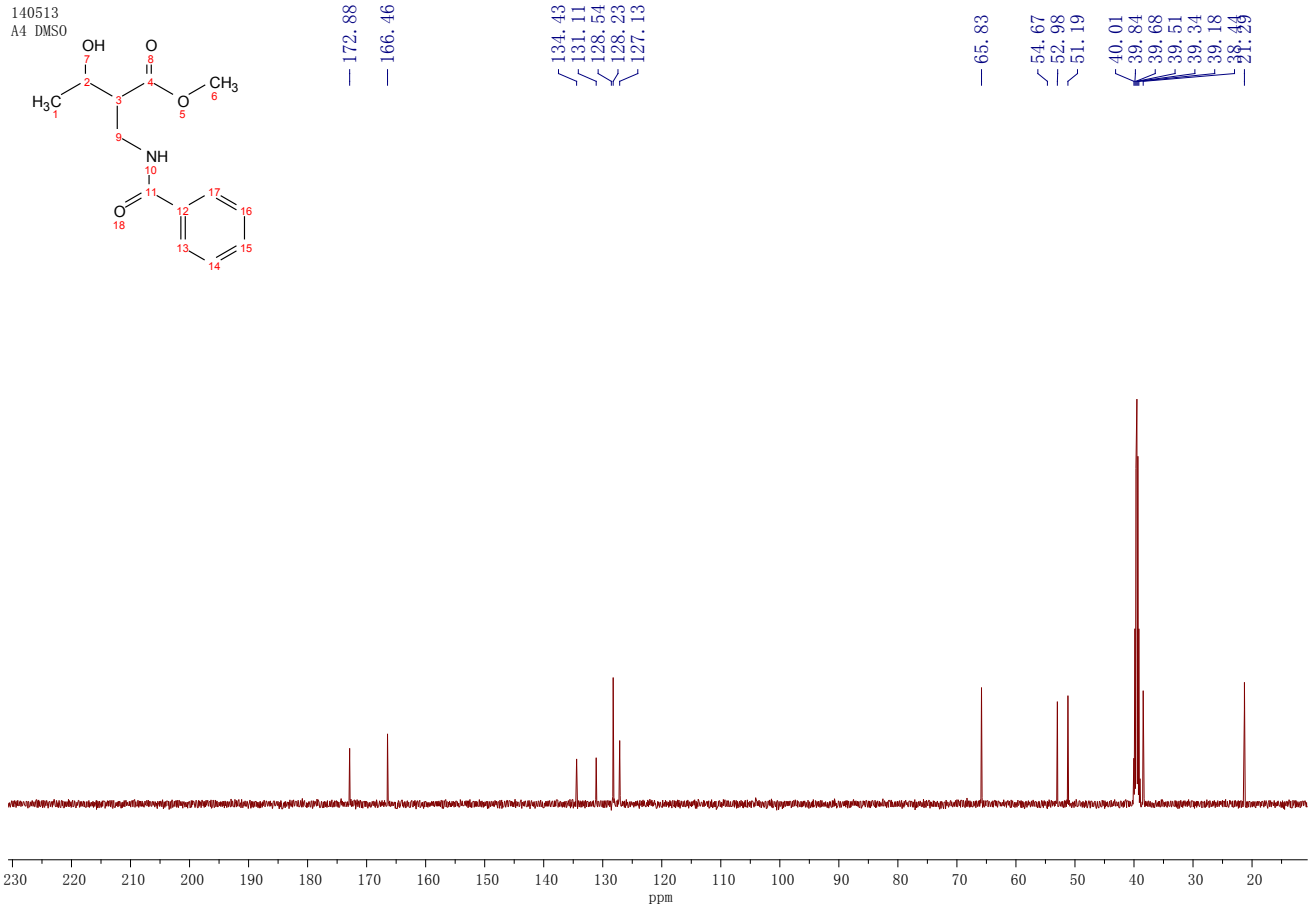

Figure S36. ^{13}C NMR spectrum of MBHB synthesized by $NaBH_4$ reduction (126 MHz, DMSO-d_6).

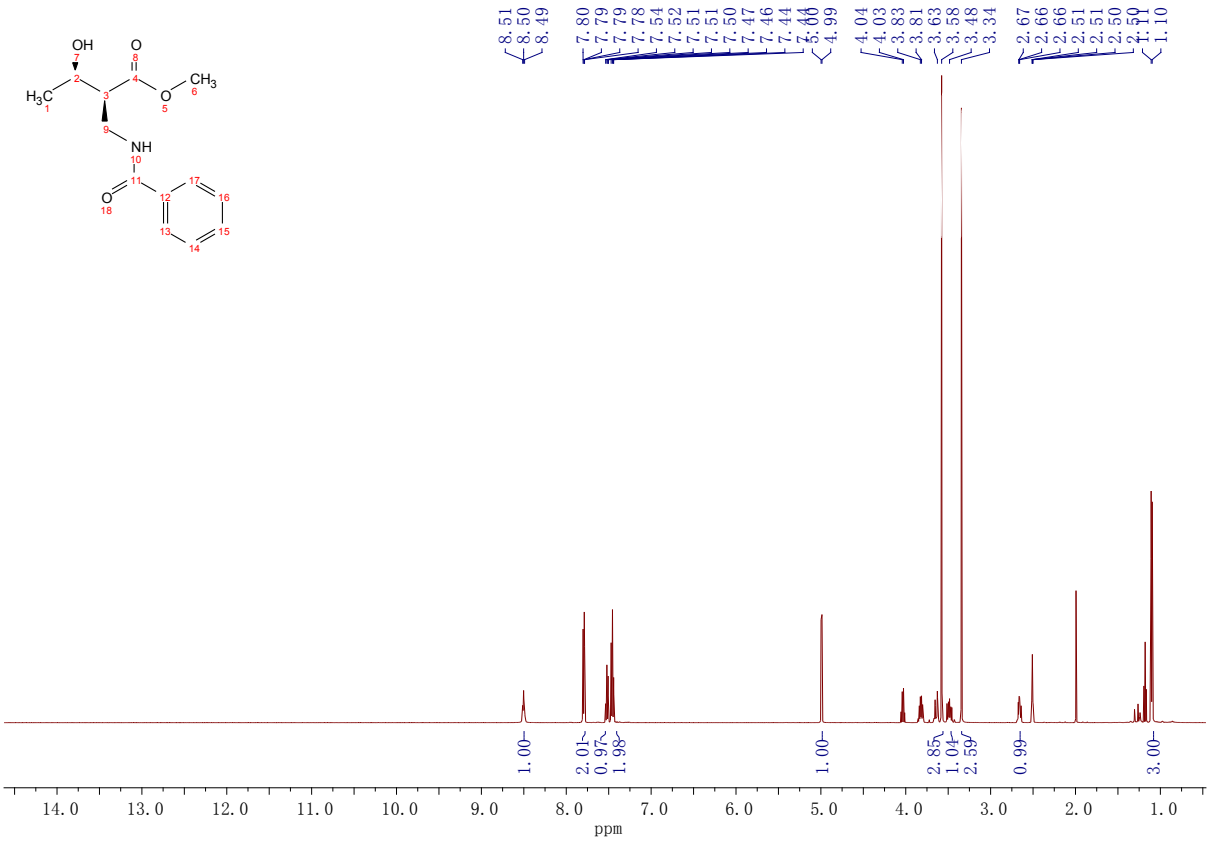

Figure S37. ^{1}H NMR spectrum of biotransformation product (*2S, 3R*)-MBHB (500 MHz, DMSO-d_6).

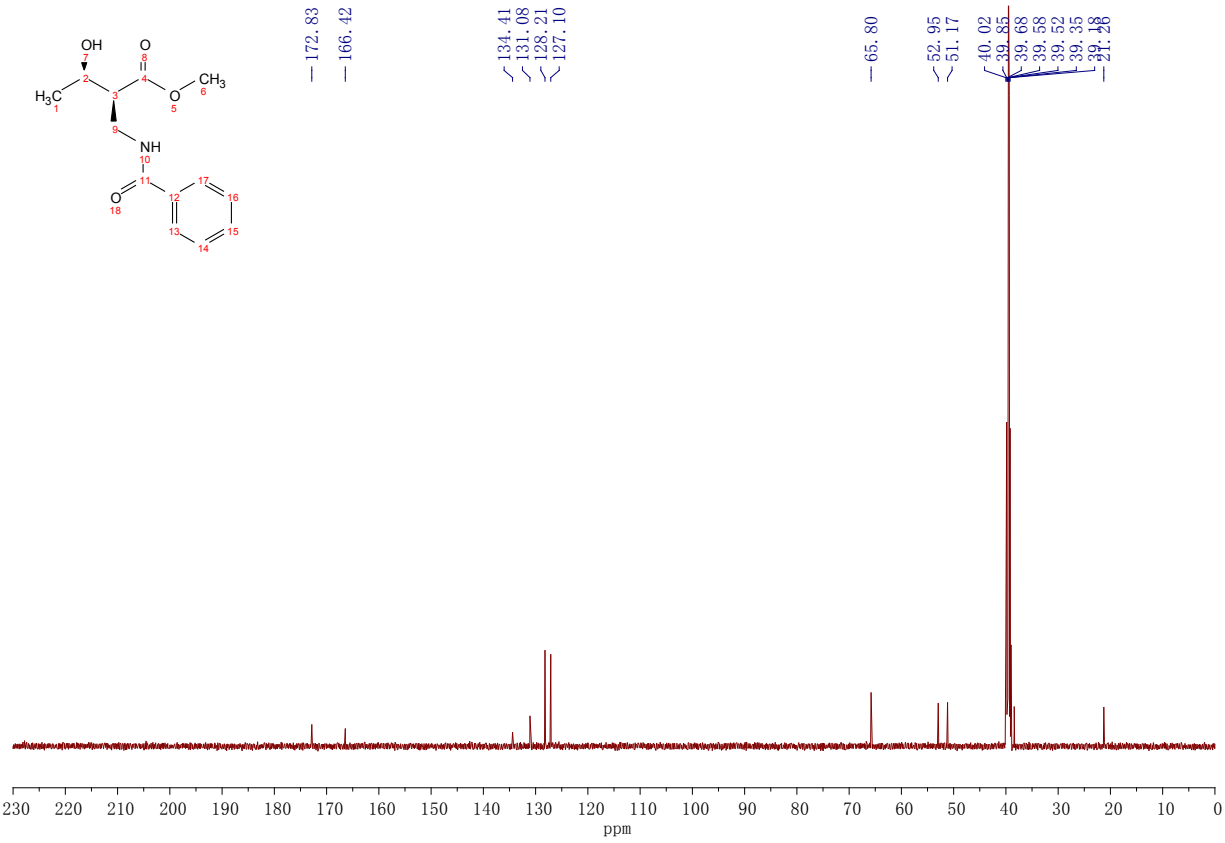

Figure S38. ^{13}C NMR spectrum of biotransformation product (*2S, 3R*)-MBHB (126 MHz, DMSO-d_6).

19. References

1 A. Mateska, G. Stojkovic, B. Mikova, K. Mladenovska, E. Popovski, *ARKIVOC* 2009, **x**, 131; M. Chao, A. Hao, H. Wang, *Org. Process. Res. Dev.* 2009, **13**, 645.

2 Y. Nie, R. Xiao, Y. Xu, G. T. Montelione, *Org. Biomol. Chem.* 2011, **9**, 4070; Z. Y. You, Z. Q. Liu, Y. G. Zheng, *Appl. Microbiol. Biot.* 2014, **98**, 1671.

3 C. T. Chung, S. L. Niemela, R. H. Miller, *Proc. Natl. Acad. Sci.* 1989, **86**, 2172.

4 Z. Q. Liu, P. J. Baker, F. Cheng, Y. P. Xue, Y. G. Zheng, Y. C. Shen, *Plos One* 2013, **8**, 1.

5 Y. Nakamura, T. Gojobori, T. Ikemura, *Nucleic. Acids. Res.* 2000, **28**, 292.

6 X. Chen, Y. G. Zheng, Z. Q. Liu, L. H. Sun, *J. Chromatogr. B* 2015, **974**, 57.

7 P. Gouet, X. Robert, E. Courcelle, *Nucleic. Acids. Res.* 2003, **31**, 3320.

8 A. Lerchner, A. Jarasch, W. Meining, A. Schiefner, A. Skerra, *Biotechnol. Bioeng.* 2013, **110**, 2803; N. H. Schlieben, K. Niefind, J. Muller, B. Riebel, W. Hummel, D. Schomburg, *J. Mol. Biol.* 2005, **349**, 801; A. Fiser, A. Sali, *Macromolecular Crystallography, Pt D* 2003, **374**, 461.

9 F. Osterberg, G. M. Morris, M. F. Sanner, A. J. Olson, D. S. Goodsell, *Proteins* 2002, **46**, 34.